A VERSATILE TRIVARIATE WRAPPED CAUCHY COPULA WITH APPLICATIONS TO TOROIDAL AND CYLINDRICAL DATA

A PREPRINT

Shogo Kato
Institute of Statistical Mathematics
Tokyo
Japan
skato@ism.ac.jp

Christophe Ley
Department of Mathematics
University of Luxembourg
Luxembourg
christophe.ley@uni.lu

Sophia Loizidou
Department of Mathematics
University of Luxembourg
Luxembourg
sophia.loizidou@uni.lu

Kanti V. Mardia
Department of Statistics
University of Leeds
United Kingdom
k.v.mardia@leeds.ac.uk

October 14, 2024

ABSTRACT

In this paper, we propose a new flexible distribution for data on the three-dimensional torus which we call a trivariate wrapped Cauchy copula. Our trivariate copula has several attractive properties. It has a simple form of density and is unimodal. its parameters are interpretable and allow adjustable degree of dependence between every pair of variables and these can be easily estimated. The conditional distributions of the model are well studied bivariate wrapped Cauchy distributions. Furthermore, the distribution can be easily simulated. Parameter estimation via maximum likelihood for the distribution is given and we highlight the simple implementation procedure to obtain these estimates. We compare our model to its competitors for analysing trivariate data and provide some evidence of its advantages. Another interesting feature of this model is that it can be extended to cylindrical copula as we describe this new cylindrical copula and then gives its properties. We illustrate our trivariate wrapped Cauchy copula on data from protein bioinformatics of conformational angles, and our cylindrical copula using climate data related to buoy in the Adriatic Sea. The paper is motivated by these real trivariate datasets, but we indicate how the model can be extended to multivariate copulas.

Keywords Angular data · copula · directional statistics · flexible modeling · wrapped Cauchy distribution

1 Introduction

Angular data occurs frequently in domains such as environmental sciences (e.g., wind directions, wave directions), bioinformatics (dihedral angles in protein backbone structures), zoology (animal movement studies), medicine (circadian body clock, secretion times of hormones), or political/social sciences (times of crimes during the day), see for example [38]. However, dealing with data that are angles requires special care in order to take into account their topology (domain $[0, 2\pi)$ where the end points coincide). Classical statistical concepts from the real line no longer hold for such data [21, 45]; in particular, the building blocks of statistical modeling and inference, probability distributions, need to be properly defined. For data involving a single angle, called circular data, a large body of literature proposing circular distributions exists (see for example [46] and [53]), among which the popular von Mises, wrapped Cauchy and cardioid models. Though less in number, there also exist several interesting distributions for data consisting respectively of two angles, called toroidal data, and an angle and a linear part, called cylindrical data. Popular examples for toroidal distributions are the bivariate von Mises [41], the Sine [57] and Cosine models [48] and the bivariate wrapped Cauchy

[31], while examples for cylindrical models are the Johnson–Wehrly [25], the Mardia–Sutton [40], the Kato–Shimizu [32] and the Abe–Ley [1] distributions.

The situation is very different when the data consists of either three angles, two angles and one linear component, or one angle and two linear components. The few existing proposals suffer from problems of tractability, complex parameter estimation procedures, lack of practically usable random number generation or non-interpretable parameters (see Section 6 for details). However, many such datasets exist which require an adequate statistical treatment. Two important examples are the following, which we will be dealing with in this paper:

- Predicting the three-dimensional folding structure of a protein from its known one-dimensional amino acid structure is among the most important yet hardest scientific challenges, with impacts in drug development, vaccine design, disease mechanism understanding, human cell injection, and enzyme engineering, to cite but these. The recent Nature Methods paper [35] concretely stated the need to complement the famous AlphaFold single point prediction with an adequate statistical uncertainty treatment: "distributions of conformations are the future of structural biology" (see our Section 7.1 for details). So far most statistical advances, in particular on flexible and tractable probability distributions, have considered the two dihedral angles ϕ and ψ, and considered the torsion angle of the side chain ω to be fixed at either 0 or π (which are the only two realistic values for this angle). However in practice this angle ω is often measured with some noise, hence a model for ϕ, ψ and ω is required.

- Many environmental agencies are collecting data on wave heights and directions in order to identify sea regimes. Such identification is highly relevant in climate-change for studies of, for instance, the drift of floating objects and oil spills, coastal erosion, and the design of off-shore structures. Typically, data analysis procedures use cylindrical distributions (e.g., the Abe–Ley distribution in [34]) to jointly model wave height and direction. A more scientifically strategic way is to add as additional variable the wind direction as it heavily influences waves. Quoting [34],"In wintertime, relevant events in the Adriatic Sea are typically generated by the southeastern Sirocco wind and the northern Bora wind". This implies adding a second angle to the cylindrical data on waves.

In order to fill this important gap in the literature, we propose in this paper the trivariate wrapped Cauchy copula. By their very nature, copula-based approaches are tailor-made for versatility as copulas are distributions (with uniform marginals) which regulate the dependence structure and can be combined with user-chosen marginals to form highly flexible new models. Indeed, from Sklar's Theorem [58] we know that any multivariate (on $\mathbb{R}^d$) cumulative distribution function (cdf) F can be expressed under the form $F(x_1, \ldots, x_d) = C(F_1(x_1), \ldots, F_d(x_d))$ with C a d-dimensional copula and $F_1, \ldots, F_d$ marginal univariate cdfs, and conversely any copula C can be combined with marginals to produce a multivariate distribution. Well-known references on copulas include [22], [52] and [23]. Copula models have successfully been used in numerous domains such as medicine, finance, actuarial sciences, hydrology or environmental sciences, see e.g. [13], [39], [7], among many others. In the case of angular data, copulas need to fulfil the additional condition of 2π-periodicity and their marginals are not uniform on $[0, 1]$ but on the unit circle. Our construction will be such that linear marginals are also admissible, in order to also cover cylindrical data. We attract the reader's attention to the fact that [26] coined the term *circulas* for copulas on the torus. In this paper we shall consistently use the word copula since our model also covers linear marginals.

Our trivariate wrapped Cauchy copula has the following further benefits: (i) simple form of density, (ii) adjustable degree of dependence between the variables, (iii) interpretable and well-estimatable parameters, (iv) well-known conditional distributions, (v) a simple data generating mechanism, and (vi) unimodality. Thus we are proposing a new model that satisfies the requirements as laid out in [36]: versatility (ability to exhibit distinct shapes), tractability, parameter interpretability, (ideally simple) data generation mechanism, and fast parameter estimation procedure. Since our model allows for linear marginals, it not only covers toroidal data but also cylindrical data, unlike the toroidal competitor models from the literature.

The paper is organized as follows. In Section 2 we review some well-known bivariate distributions which are relevant for our construction before proposing the trivariate wrapped Cauchy copula. In Section 3, several properties of the proposed distribution are given, including conditional distributions, random variate generation, unimodality and moments. Parameter estimation is considered in Section 4 and the use of non-uniform marginal distributions in Section 5. A thorough comparison with the competitors in the existing literature is given in Section 6 and in Section 7 the two real datasets described above are investigated by means of our methodology; the first about protein dihedral angles and the second about data obtained by a buoy in the Adriatic Sea. Finally, Section 8 ends with a discussion and outlook on future research. In the Appendix, the proofs of all the Theorems and Propositions in the paper are given, along with the expected Fisher Information matrix, additional plots, Monte Carlo simulation results for Section 4, further results for the protein dataset from Section 7.1, and a generalization of our model mentioned in Section 8.

2 Construction and definition of the proposed copula

Before we introduce our trivariate wrapped Cauchy copula, we will first review the most popular bivariate circular distributions.

2.1 Bivariate circular probability distributions and copulas

A popular class of toroidal (circular-circular) distributions that allows specifying the marginal distributions has been put forward by Wehrly and Johnson (1980) [60]. Their general families have the probability density functions

$$f(\theta_1, \theta_2) = 2\pi g[2\pi\{F_1(\theta_1) - F_2(\theta_2)\}]f_1(\theta_1)f_2(\theta_2), \tag{1}$$

$$f(\theta_1, \theta_2) = 2\pi g[2\pi\{F_1(\theta_1) + F_2(\theta_2)\}]f_1(\theta_1)f_2(\theta_2), \tag{2}$$

where $0 \leq \theta_1, \theta_2 < 2\pi$, f_1 and f_2 are specified densities on the circle $[0, 2\pi)$, F_1 and F_2 are their distribution functions defined with respect to fixed, arbitrary, origins, and g is also a specified density on the circle. Both families (1) and (2) have the nice property that their marginal densities are given by f_1 and f_2. More precisely, let a bivariate circular random vector (Θ_1, Θ_2) have the distribution (1) or (2). Then the marginal densities of Θ_1 and Θ_2 are given by f_1 and f_2, respectively. Note that expression (1) with θ_2 replaced by $x \in \mathbb{R}$ (and accordingly f_2 and F_2 are densities and distribution functions on $\mathbb{R}$) had been proposed by Johnson and Wehrly (1978) [25] to build general circular-linear distributions with specified marginals.

The two families (1) and (2) can be readily transformed into copulas for bivariate circular data, assuming $(U_1, U_2)' = (2\pi F_1(\Theta_1), 2\pi F_2(\Theta_2))'$. Then the density of $(U_1, U_2)'$ is given by

$$c(u_1, u_2) = \frac{1}{2\pi}g(u_1 - qu_2), \quad 0 \leq u_1, u_2 < 2\pi, \tag{3}$$

where we now write $q = 1$ if $(\Theta_1, \Theta_2)'$ has the density (1) and $q = -1$ if $(\Theta_1, \Theta_2)'$ has the density (2). Simple integration shows that $c(u_1, u_2)$ integrates to 1 and that each marginal is uniform on the circle (see [26] for further properties of the distribution (3)). Therefore the distribution (3) can be viewed as an equivalent of a copula for bivariate circular data. From Sklar's theorem (see page 18 in [52]), the distribution with density (3) can be transformed into a distribution with prespecified marginal distributions. The distributions of Wehrly and Johnson (1) and (2) are such cases in which the marginal distributions have the continuous distributions with densities f_1 and f_2.

In practice, it is necessary to take specific densities for f_1, f_2 and g in the families of Wehrly and Johnson, or equivalently, the choice of g and marginal distributions is important for the copula-based version (3). Various proposals have been put forward in the literature, many of which are based on the use of the von Mises distribution, for example in [60], [55] and [56]. Using a different approach, [8] applied the densities based on non-negative trigonometric sums. We refer the reader to [37], Section 2.4, for a review of these models. Further, [29] and [31] adopted the wrapped Cauchy density as the function g in (3). This leads to density (3) being of the form

$$c(u_1, u_2) = \frac{1}{4\pi^2}\frac{|1 - \rho^2|}{1 + \rho^2 - 2\rho\cos(u_1 - u_2 - \mu)}, \quad 0 \leq u_1, u_2 < 2\pi, \tag{4}$$

where $\mu \in [0, 2\pi)$ is the location parameter and $\rho \in \mathbb{R} \setminus \{\pm 1\}$ the dependence parameter between the two variables. The distribution (4) is called a bivariate wrapped Cauchy copula which we label as $\mathrm{BWC}(\mu, \rho)$. In fact, [29] showed that this distribution is derived from a problem in Brownian motion and possesses various tractable properties. Moreover, [31] transformed this model via the Möbius transformation and showed that the transformed distribution (known as Kato–Pewsey model) has the wrapped Cauchy marginal and conditional distributions.

2.2 Our proposal: the trivariate wrapped Cauchy copula

Knowing these attractive properties of the bivariate wrapped Cauchy distribution of [31] resulting from the copula (4), we extend (4) to a density on the three-dimensional torus in the following theorem.

Theorem 1. *For $\boldsymbol{u} = (u_1, u_2, u_3)'$ and $\boldsymbol{\rho} = (\rho_{12}, \rho_{13}, \rho_{23})'$, let*

$$t(\boldsymbol{u}; \boldsymbol{\rho}) = c_2\Big[c_1 + 2\{\rho_{12}\cos(u_1 - u_2) + \rho_{13}\cos(u_1 - u_3) + \rho_{23}\cos(u_2 - u_3)\}\Big]^{-1}, \tag{5}$$

$$0 \leq u_1, u_2, u_3 < 2\pi,$$

where $\rho_{12}, \rho_{13}, \rho_{23} \in \mathbb{R} \setminus \{0\}$, $\rho_{12}\rho_{13}\rho_{23} > 0$,

$$c_1 = \frac{\rho_{12}\rho_{13}}{\rho_{23}} + \frac{\rho_{12}\rho_{23}}{\rho_{13}} + \frac{\rho_{13}\rho_{23}}{\rho_{12}}, \tag{6}$$

3

and

$$c_2 = \frac{1}{(2\pi)^3} \left\{ \left(\frac{\rho_{12}\rho_{13}}{\rho_{23}}\right)^2 + \left(\frac{\rho_{12}\rho_{23}}{\rho_{13}}\right)^2 + \left(\frac{\rho_{13}\rho_{23}}{\rho_{12}}\right)^2 - 2\rho_{12}^2 - 2\rho_{13}^2 - 2\rho_{23}^2 \right\}^{1/2}. \tag{7}$$

Suppose that there exists one of the permutations of $(1,2,3)$, (i,j,k), such that

$$|\rho_{jk}| < |\rho_{ij}\rho_{ik}|/(|\rho_{ij}| + |\rho_{ik}|), \tag{8}$$

where $\rho_{ji} = \rho_{ij}$ for $1 \leq i < j \leq 3$. Then the function (5) is a probability density function on the three-dimensional torus $[0, 2\pi)^3$. Its parameters $\boldsymbol{\rho}$ are not identifiable but without loss of generality we take our identifiability constraint given by

$$\rho_{12}\rho_{13}\rho_{23} = 1. \tag{9}$$

Proof. See Section A.2 in the Appendix for the proof that function (5) is a density under the positivity condition given by (8). We can show that the model is not identifiable by noting that $t(\boldsymbol{u}; \boldsymbol{\rho}) = t(\boldsymbol{u}; c\boldsymbol{\rho})$ for any constant $c \in \mathbb{R}^+$ and the condition (9) takes that into account. $\square$

We will refer to this distribution, which has the density of $(U_1, U_2, U_3)'$ given by (5), as the trivariate wrapped Cauchy copula (TWCC or TWC copula). The distribution (5) is also denoted by TWCC($\boldsymbol{\rho}$) in order to specify its parameters. In TWCC, different functions of parameters ρ_{12}, ρ_{13} and ρ_{23} control the dependence between the U_i's and the location of the modes, see Theorems 6 and 7 in Section 3. More discussion about the interpretation of the parameters will be given in Section 3.6. It is also straightforward to incorporate both positive and negative associations by replacing u_i with $q_i u_i$ ($q_i = 1, -1$) and it is possible to extend the distribution to include location parameters by replacing $u_i - u_j$ with $u_i - u_j - \mu_{ij}$ in (5) ($0 \leq \mu_{ij} < 2\pi$). Although the parametrization used in the expression (5) for the density is natural in the sense that each parameter ρ_{ij} is multiplied by a function of $u_i - u_j$, this expression does not allow for the independence between U_i and U_j. However, an alternative parametrization is available that accommodates the independence between the variables; see equation (13) below. A very appealing aspect from both a tractability and computational viewpoint is the closed form of the density which does not include any integrals or infinite sums, unlike most existing distributions on the three-dimensional torus (see Section 6).

Note that condition (8) can be re-expressed under simpler form as $\rho_{ij}^2 \rho_{ik}^2 > (|\rho_{ij}| + |\rho_{ik}|)$ under (9). The following result formally establishes the identifiability of the parameters in our model.

Proposition 1. *The TWCC density (5) has identifiable parameters.*

Proof. See Section A.3 in the Appendix. $\square$

Next, we show that our model given by TWCC is indeed a copula for trivariate circular data by establishing in Theorem 2 that its univariate marginals are circular uniform distributions. Prior to this, we will show that the bivariate marginals of our new model are bivariate wrapped Cauchy-type copulas as they are of the form (4).

Theorem 2. *Let a trivariate circular random vector $(U_1, U_2, U_3)'$ follow the TWCC with density (5). Then the following hold for the marginal distributions of $(U_1, U_2, U_3)'$:*

(i) The marginal distribution of $(U_i, U_j)'$ is of the form (4) with density

$$t_2(u_i, u_j; \phi_{ij}) = \frac{1}{4\pi^2} \frac{|1 - \phi_{ij}^2|}{1 + \phi_{ij}^2 - 2\phi_{ij}\cos(u_i - u_j)}, \quad 0 \leq u_i, u_j < 2\pi, \tag{10}$$

where

$$\phi_{ij} = \frac{1}{2\rho_{ij}} \left\{ \frac{\rho_{ik}\rho_{jk}}{\rho_{ij}} - \frac{\rho_{ij}\rho_{ik}}{\rho_{jk}} - \frac{\rho_{ij}\rho_{jk}}{\rho_{ik}} - (2\pi)^3 c_2 \right\}, \tag{11}$$

and c_2 is as in (7).

(ii) The marginal distribution of U_i is the uniform distribution on the circle with density

$$t_1(u_i) = \frac{1}{2\pi}, \quad 0 \leq u_i < 2\pi.$$

Therefore the distribution of $(U_1, U_2, U_3)'$ is a copula for trivariate circular data.

Proof. See Section A.4 in the Appendix. $\square$

Note that the ϕ_{ij} are invariant under ρ_{ij} replaced by $c\rho_{ij}$ for some constant $c \in \mathbb{R}^+$, implying that they do not depend on any identifiability condition on ρ_{ij}. We draw the reader's attention to the fact that the constant c_1 has to be of the form (6), which guarantees that the bivariate marginal distribution belongs to the bivariate wrapped Cauchy-type family. See equality (41) in the proof of Theorem 2(i).

Finally, note that the TWCC density given by (5) can also be expressed as

$$\tilde{t}(\boldsymbol{u}; \boldsymbol{\rho}) = \tilde{c}_2 \Big[\tilde{c}_1 + 2\rho_{12}\rho_{13}\rho_{23} \left\{ \rho_{12} \cos(u_1 - u_2) + \rho_{13} \cos(u_1 - u_3) + \rho_{23} \cos(u_2 - u_3) \right\} \Big]^{-1}, \qquad (12)$$

where $\tilde{c}_1 = (\rho_{12}\rho_{13})^2 + (\rho_{12}\rho_{23})^2 + (\rho_{13}\rho_{23})^2$ and

$$\tilde{c}_2 = \frac{1}{(2\pi)^3} \left\{ (\rho_{12}\rho_{13})^4 + (\rho_{12}\rho_{23})^4 + (\rho_{13}\rho_{23})^4 - 2\rho_{12}^2\rho_{13}^2\rho_{23}^2(\rho_{12}^2 + \rho_{13}^2 + \rho_{23}^2) \right\}^{1/2}.$$

This form of the density has the advantage that it does not require the conditions $\rho_{12}\rho_{13}\rho_{23} > 0$ because of the equality $\tilde{t}(\boldsymbol{u}; \boldsymbol{\rho}) = \tilde{t}(\boldsymbol{u}; -\boldsymbol{\rho})$ for any $\rho_{12}\rho_{13}\rho_{23} > 0$.

3 Properties of the TWC copula

We will investigate distinct properties of our new copula distribution TWCC($\boldsymbol{\rho}$). In order to do so, it is often convenient to express its density using complex variables. Let $(U_1, U_2, U_3)'$ have the TWCC density (5), and assume that $(Z_1, Z_2, Z_3)' = (e^{iU_1}, e^{iU_2}, e^{iU_3})'$. Then some simple algebra yields that the TWCC density can be expressed as

$$tc(\boldsymbol{z}; \boldsymbol{\phi}) = \frac{1}{(2\pi)^3} \frac{\{\phi_1^4 + \phi_2^4 + \phi_3^4 - 2\phi_1^2\phi_2^2 - 2\phi_1^2\phi_3^2 - 2\phi_2^2\phi_3^2\}^{1/2}}{|\phi_1 z_1 + \phi_2 z_2 + \phi_3 z_3|^2}, \quad \boldsymbol{z} = (z_1, z_2, z_3)' \in \Omega, \qquad (13)$$

where $\Omega = \{z \in \mathbb{C} \,;\, |z| = 1\}$ is the unit circle in the complex plane and $\boldsymbol{\phi} = (\phi_1, \phi_2, \phi_3)'$ with

$$\phi_1 = \operatorname{sgn}(\rho_{23}) \left| \frac{\rho_{12}\rho_{13}}{\rho_{23}} \right|^{1/2}, \quad \phi_2 = \operatorname{sgn}(\rho_{13}) \left| \frac{\rho_{12}\rho_{23}}{\rho_{13}} \right|^{1/2}, \quad \phi_3 = \operatorname{sgn}(\rho_{12}) \left| \frac{\rho_{13}\rho_{23}}{\rho_{12}} \right|^{1/2}. \qquad (14)$$

We call this the complex TWCC. Note that, in terms of the original parameters, we have $\rho_{12} = \phi_1\phi_2$, $\rho_{13} = \phi_1\phi_3$ and $\rho_{23} = \phi_2\phi_3$. The inequality (8) on the parameters in Theorem 1 then simplifies to $|\phi_i| > |\phi_j| + |\phi_k|$ for (i, j, k) a certain permutation of $(1, 2, 3)$. In fact, this is equivalent to the condition that the denominator of (13) satisfies $\phi_1 z_1 + \phi_2 z_2 + \phi_3 z_3 \neq 0$ for all $(z_1, z_2, z_3)'$, see Lemma 1 in Section A.1 of the Appendix for a statement and proof. Equivalently, the condition on the parameter $|\rho_{jk}| < |\rho_{ij}\rho_{ik}|/(|\rho_{ij}| + |\rho_{ik}|)$ for some (i, j, k) is necessary to guarantee the boundedness of the TWCC($\boldsymbol{\rho}$) for all $(u_1, u_2, u_3)'$. The identifiability constraint (9) turns into $(\phi_1\phi_2\phi_3)^2 = 1$. Note that the parameter space of the complex TWCC must satisfy $|\phi_i| > |\phi_j| + |\phi_k|$, but the identifiability condition can be extended from $(\phi_1\phi_2\phi_3)^2 = 1$ to include $\phi_k = 0$, which implies independence between Z_k and the other variables.

3.1 Conditional distributions and regression

In this subsection we consider the conditional distributions of the model TWCC($\boldsymbol{\rho}$). As we will show, just like the bivariate and univariate marginal distributions, all conditional distributions belong to well-known families, namely to wrapped Cauchy distributions on the circle and to the Kato–Pewsey distribution on the torus. This property also highlights the versatility of the TWCC.

Theorem 3. *Let $(U_1, U_2, U_3)'$ be a trivariate random vector having the distribution TWCC($\boldsymbol{\rho}$). Then the conditional distributions of $(U_1, U_2, U_3)'$ are given below.*

(i) *The conditional distribution of $(U_i, U_j)'$ given $U_k = u_k$ is a reparametrized version of the distribution of [31] with density*

$$t_{2|1}(u_i, u_j | u_k; \boldsymbol{\rho})$$
$$= 2\pi c_2 \Big[c_1 + 2 \left\{ \rho_{ij} \cos(u_i - u_j) + \rho_{ik} \cos(u_i - u_k) + \rho_{jk} \cos(u_j - u_k) \right\} \Big]^{-1}, \qquad (15)$$

or, equivalently in the form of the bivariate Cauchy distribution,

$$= 2\pi c_2 \Big[c_1 + 2\{ \rho_{ik} \cos(u_i - u_k) + \rho_{jk} \cos(u_j - u_k)$$
$$+ \rho_{ij} \cos(u_i - u_k) \cos(u_j - u_k) + \rho_{ij} \sin(u_i - u_k) \sin(u_j - u_k) \} \Big]^{-1}, \qquad (16)$$
$$0 \leq u_i, u_j < 2\pi.$$

(ii) The conditional distribution of U_i given $U_j = u_j$ is the wrapped Cauchy distribution with density

$$t_{1|1}(u_i|u_j; \phi_{ij}) = \frac{1}{2\pi} \frac{|1 - \phi_{ij}^2|}{1 + \phi_{ij}^2 - 2\phi_{ij}\cos(u_i - u_j)}, \quad 0 \le u_i < 2\pi, \tag{17}$$

where ϕ_{ij} is as in (11).

(iii) The conditional distribution of U_i given $(U_j, U_k)' = (u_j, u_k)'$ is the wrapped Cauchy distribution with density

$$t_{1|2}(u_i|u_j, u_k; \delta_{i|jk}) = \frac{1}{2\pi} \frac{|1 - \delta_{i|jk}^2|}{1 + \delta_{i|jk}^2 - 2\delta_{i|jk}\cos(u_i - \eta_{i|jk})}, \quad 0 \le u_i < 2\pi, \tag{18}$$

where for $\phi_{i|jk} = -\rho_{jk}(\rho_{ik}^{-1}e^{iu_j} + \rho_{ij}^{-1}e^{iu_k})$,

$$\eta_{i|jk} = \arg(\phi_{i|jk}) \quad and \quad \delta_{i|jk} = |\phi_{i|jk}|. \tag{19}$$

Proof. See Section A.5 in the Appendix. □

As this theorem shows, the univariate conditionals in Theorem 3(ii) and (iii) have the wrapped Cauchy distributions. Note that the univariate conditional given in Theorem 3(ii) does not follow the wrapped Cauchy in general if c_1 is not defined as in (6). The bivariate conditional in Theorem 3(i) has various tractable properties as discussed in [31].

The well-known form of the conditional distributions paves the way for regression purposes with one or two angular dependent variables and/or one or two angular regressors. Indeed, if we wish to predict one angular component based on two angular components, then from Theorem 3(iii) we find that the mean direction and circular variance of (U_i) given $(U_j, U_k)'$ are simply $\eta_{i|jk}$ and $1 - \delta_{i|jk}$, respectively. Similarly, if we wish to predict two angular components based on a third angular component, then from Theorem 3(i) we see that the toroidal mean and variance of $(U_i, U_j)'$ given U_k can be calculated in the same way as in Section 2.5 of [31]. Note that circular-circular regression of, for example, U_i given U_j can also be obtained in a straightforward way from Theorem 3(ii). These properties are not explored here but we emphasize that they can be used in practice easily.

3.2 Random variate generation

The fact that all the marginal and conditional distributions belong to existing tractable families lays the foundations for random variate generation. Indeed, random variates from the proposed trivariate model $\text{TWCC}(\boldsymbol{\rho})$ can be efficiently generated from uniform random variates on $(0, 1)$, as detailed in the following theorem.

Theorem 4. *The following algorithm generates random variates from the distribution $TWCC(\boldsymbol{\rho})$ without rejection.*

Step 1. Generate uniform $(0, 1)$ random variates ω_1, ω_2 and ω_3.

Step 2. Compute

$$u_1 = 2\pi\omega_1, \quad u_2 = u_1 + \arg(\phi_{12}) + 2\arctan\left[\left(\frac{1 - |\phi_{12}|}{1 + |\phi_{12}|}\right)\tan\{\pi(\omega_2 - 0.5)\}\right],$$

$$u_3 = \eta_{3|12} + 2\arctan\left[\left(\frac{1 - \delta_{3|12}}{1 + \delta_{3|12}}\right)\tan\{\pi(\omega_3 - 0.5)\}\right],$$

where ϕ_{12} is as in (11) and $(\eta_{3|12}, \delta_{3|12})$ are as in (19).

Step 3. Output $(u_1, u_2, u_3)'$ as the random variate from the distribution $TWCC(\boldsymbol{\rho})$.

Proof. See Section A.6 in the Appendix. □

We note the simplicity and efficiency of the algorithm in which a variate from the proposed distribution can be generated through a transformation of three uniform random variates without rejection.

3.3   Trigonometric moments

For a trivariate circular random vector $(U_1, U_2, U_3)'$, its trigonometric moment of order $(p_1, p_2, p_3)'$ is defined by

$$\Phi(p_1, p_2, p_3) = E\left[e^{\mathrm{i}(p_1 U_1 + p_2 U_2 + p_3 U_3)}\right],$$

where $(p_1, p_2, p_3)' \in \mathbb{Z}^3$ is the order of the trigonometric moments. The following theorem shows that the trigonometric moments for the proposed distribution TWCC($\boldsymbol{\rho}$) can be expressed in simple form.

Theorem 5. *Let $(U_1, U_2, U_3)'$ have the distribution TWCC($\boldsymbol{\rho}$) with $|\rho_{jk}| < |\rho_{ij}\rho_{ik}|/(|\rho_{ij}| + |\rho_{ik}|)$. Then we have the following cases.*

(i) *If $p_1 + p_2 + p_3 \neq 0$, $\Phi(p_1, p_2, p_3) = 0$.*

(ii) *If $p_1 + p_2 + p_3 = 0$ and $p_i \geq 0$, then*

$$\Phi(p_1, p_2, p_3) = (-\rho_{jk})^{p_i} \sum_{n=0}^{p_i} \binom{p_i}{n} \rho_{ik}^{-n} \rho_{ij}^{-p_i+n} \varphi_{jk}^{|p_j+n|}, \tag{20}$$

where

$$\varphi_{jk} = \min\{|\phi_{jk}|, |\phi_{jk}|^{-1}\}\phi_{jk}/|\phi_{jk}| \tag{21}$$

and ϕ_{jk} is given by (11).

(iii) *If $p_1 + p_2 + p_3 = 0$ and $p_i \geq 0$ and*

- *if $p_j \geq 0$, then the trigonometric moment simplifies to*

$$\Phi(p_1, p_2, p_3) = \varphi_{jk}^{p_j}\left\{-\rho_{jk}\left(\frac{\varphi_{jk}}{\rho_{ik}} + \frac{1}{\rho_{ij}}\right)\right\}^{p_i};$$

- *if $p_j \leq -p_i$, then*

$$\Phi(p_1, p_2, p_3) = \varphi_{jk}^{-p_j}\left\{-\rho_{jk}\left(\frac{1}{\varphi_{jk}\rho_{ik}} + \frac{1}{\rho_{ij}}\right)\right\}^{p_i}. \tag{22}$$

(iv) *If $p_1 + p_2 + p_3 = 0$ and $p_i < 0$, then $\Phi(p_1, p_2, p_3) = \Phi(-p_1, -p_2, -p_3)$.*

(v) *If $p_1 + p_2 + p_3 = 0$ and $p_i = 0$, the trigonometric moment is given by*

$$\Phi(p_1, p_2, p_3) = \varphi_{jk}^{|p_j|}.$$

Proof. See Section A.7 in the Appendix.   □

We note that Theorem 5(i) is not specific to the TWCC distribution and can be generalized to a more general multivariate family. For details, see Theorem 9(ii). We will come back to these results when we deal with the parameter estimation by the method of moments in Section 4.1.

3.4   Correlation coefficients

We consider three well-known correlation coefficients for bivariate circular data. Let $(U_i, U_j)'$ be a bivariate circular random vector and $X_k = (\cos U_k, \sin U_k)'$ $(k = i, j)$. Then the correlation coefficients of Johnson and Wehrly [24], Jupp and Mardia [27] and Fisher and Lee [11] are respectively defined by

$$\rho_{\mathrm{JW}} = \lambda^{1/2}, \quad \rho_{\mathrm{JM}} = \mathrm{tr}(\Sigma_{ii}^{-1}\Sigma_{ij}\Sigma_{jj}^{-1}\Sigma_{ij}^T),$$

$$\rho_{\mathrm{FL}} = \frac{\det\{E(X_i X_j')\}}{[\det\{E(X_i X_i')\}\det\{E(X_j X_j')\}]^{1/2}},$$

where λ is the largest eigenvalue of $\Sigma_{ii}^{-1}\Sigma_{ij}\Sigma_{jj}^{-1}\Sigma_{ij}'$ and $\Sigma_{k\ell} = E(X_k X_\ell') - E(X_k)E(X_\ell)'$ $(k, \ell = i, j)$. The correlation coefficients of our bivariate marginal distributions are given in the following theorem.

7

Theorem 6. *Let a trivariate random vector $(U_1, U_2, U_3)'$ follow the model TWCC($\boldsymbol{\rho}$). Then, for any pair of random variables $(U_i, U_j)'$, its correlation coefficients of Johnson and Wehrly [24], Jupp and Mardia [27] and Fisher and Lee [11] are given by*

$$\rho_{\mathrm{JW}} = |\phi_{ij}|, \quad \rho_{\mathrm{JM}} = 2\phi_{ij}^2 \quad \textit{and} \quad \rho_{\mathrm{FL}} = \phi_{ij}^2,$$

respectively, where ϕ_{ij} is given in (11).

Proof. See Section A.8 in the Appendix. □

Note the simplicity of the expressions for all the three correlation coefficients. Further these all depend on the parameter ϕ_{ij}, implying that it is a good measure of dependence of the model. Recall in this context the agreeable fact that ϕ_{ij} remains invariant under ρ_{ij} being replaced by $c\rho_{ij}$ for some constant c, hence does not depend on the identifiability condition on ρ_{ij}.

3.5 Modality

In this section we investigate the modes of TWCC($\boldsymbol{\rho}$).

Theorem 7. *For $\rho_{ij} > 0$ and $\rho_{ik}, \rho_{jk} < 0$, the modes of the density TWCC($\boldsymbol{\rho}$) are given by*

$$
\begin{array}{llll}
(i) & u_i = u_j = u_k & \textit{if } |\rho_{ij}| < |\rho_{ik}\rho_{jk}|/(|\rho_{ik}| + |\rho_{jk}|), \\
(ii) & u_i = u_j + \pi = u_k + \pi & \textit{if } |\rho_{ik}| < |\rho_{ij}\rho_{jk}|/(|\rho_{ij}| + |\rho_{jk}|),
\end{array}
\tag{23}
$$

and the antimodes of the density TWCC($\boldsymbol{\rho}$) are given by

$$u_i = u_j = u_k + \pi. \tag{24}$$

If $\rho_{ij}, \rho_{ik}, \rho_{jk} > 0$, then u_k in the modes (23) and antimodes (24) is replaced by $u_k + \pi$.

Proof. See Section A.9 in the Appendix. □

Since the conditions in (23) are the same as (8) in Theorem 1, one of them is always satisfied, which makes the result very strong as it shows that our trivariate copula is unimodal. Moreover, the modes of TWCC($\boldsymbol{\rho}$) have the most natural form in the case (i) of equation (23), and very simple forms in the other cases. This unimodality property greatly simplifies working with mixtures as can be appreciated for example in our real data application from Section 7.2.

3.6 Other properties of the TWCC density and contour plots

Here we present some other properties of the TWCC density including the limiting cases, display the contour plots, and discuss the interpretation of the parameters. We first consider limiting cases of the parameter values of TWCC($\boldsymbol{\rho}$) with the constraint on ρ_{23}, meaning

$$|\rho_{23}| < |\rho_{12}\rho_{13}|/(|\rho_{12}| + |\rho_{13}|). \tag{25}$$

Note that this order of the indices is selected without any loss of generality and can be permuted. Under this assumption, the two cases of the parameters, namely, with and without the constraint $\rho_{12}\rho_{13}\rho_{23} = 1$, are discussed.

Proposition 2. *Suppose that the positivity constraint (25) holds and that the constraint $\rho_{12}\rho_{13}\rho_{23} = 1$ does not hold in general. Then the following limiting results hold for TWCC($\boldsymbol{\rho}$):*

1. *As $\rho_{23} \to 0$, TWCC($\boldsymbol{\rho}$) converges to the uniform distribution on the torus $[0, 2\pi)^3$.*

2. *As $|\rho_{12}| \to \infty$, TWCC($\boldsymbol{\rho}$) converges to the distribution with density*

$$t(\boldsymbol{u}; \boldsymbol{\rho}) = \frac{1}{(2\pi)^3} \frac{1 - \rho_{23.13}^2}{1 + \rho_{23.13}^2 + 2\rho_{23.13}\cos(u_1 - u_2)}, \quad 0 \le u_1, u_2 \le 2\pi, \tag{26}$$

   where $\rho_{23.13} = \rho_{23}/\rho_{13}$ satisfies $|\rho_{23.13}| < 1$. Therefore the bivariate vector $(U_1, U_2)'$ of this limiting distribution is independent of U_3 (which is uniformly distributed) and follows the bivariate wrapped Cauchy copula (4) labelled BWC(0,$\rho_{23.13}$).

Proof. See Section A.10 in the Appendix. □

Note that $\rho_{23.12}$, which is referred to as a partial dependence parameter, can be interpreted as the parameter that controls the strength of dependence between U_1 and U_2 when $|\rho_{12}|$ is large. To be more specific, Proposition 2(ii) implies that if $|\rho_{23.13}| \simeq 1$, then U_1 and U_2 have a strong dependence. In particular, for any $\varepsilon > 0$ and a fixed sign of $\rho_{23.13}$, it holds that $\lim_{|\rho_{13}| \to |\rho_{23}|+0} P(|U_i - U_j - \pi I(\rho_{23.13} > 0)| < \varepsilon) \to 1$. On the other hand, if $|\rho_{23.13}| \ll 1$, then the dependence between U_1 and U_2 becomes weak. The positive and negative values of $\rho_{23.13}$ imply the modes at $u_1 = u_2 + \pi$ and at $u_1 = u_2$, respectively; see [29].

Let us define
$$T_1 = U_1 - U_2, \quad T_2 = U_2, \quad T_3 = U_3,$$

then it can be seen that T_1 is univariate wrapped Cauchy which is independent of T_2 and T_3 which are independently uniformly distributed. Now as $\rho_{23.12} \to 1$, T_1 tends to univariate Cauchy on the real line. This can be seen from the fact that with $t_1 = \epsilon v/\{2(1-\epsilon)^{1/2}\}$, $\rho_{23.12} = 1 - \epsilon$ for small $\epsilon > 0$,

$$f(t_1) = \frac{1}{2\pi}\frac{1 - \rho_{23.12}^2}{1 + \rho_{23.12}^2 - 2\rho_{23.12}\cos(t_1)} \simeq \frac{1}{2\pi}\frac{1 - \rho_{23.12}^2}{(1 - \rho_{23.12})^2 + 2\rho_{23.12}\{\epsilon^2 v^2/4(1-\epsilon)\}/2} = \frac{1}{\pi}\frac{1}{1 + v^2}.$$

Next, with the additional constraint $\rho_{12}\rho_{13}\rho_{23} = 1$, the limiting cases of our model are more involved.

Proposition 3. *Let $\{\boldsymbol{\rho}_n\}_{n=1}^{\infty}$ be a sequence of parameters of the TWCC density. Assume that $\boldsymbol{\rho}_n = (\rho_{12,n}, \rho_{13,n}, \rho_{23,n})'$ satisfies $\rho_{12,n}\rho_{13,n}\rho_{23,n} = 1$, $\rho_{12,n} = O(n^\iota)$, $\rho_{13,n} = O(n^\kappa)$, $\rho_{23,n} = O(n^\lambda)$, and $\iota \geq \kappa$. Then the following hold for TWCC($\boldsymbol{\rho}_n$):*

 (i) *If $\kappa > \lambda$, then TWCC($\boldsymbol{\rho}_n$) converges to the uniform distribution on the torus as $n \to \infty$.*

 (ii) *Let $\rho_{12,n} = a^{-1}n$, $\rho_{13,n} = n^{-1/2}$ and $\rho_{23,n} = an^{-1/2}$ $(0 < a < (-1 + \sqrt{5})/2)$. Then $\kappa = \lambda$ holds and TWCC($\boldsymbol{\rho}_n$) converges to the distribution (26) with $\rho_{23.13} = a$ as $n \to \infty$.*

Proof. See Section A.11 in the Appendix. □

Proposition 3(ii) implies that if $\kappa = \lambda$, the convergence of TWCC($\boldsymbol{\rho}_n$) as $n \to \infty$ differs depending on the specific forms of $\boldsymbol{\rho}_n$.

Now we present some more properties of the TWCC density. Their proofs are straightforward and omitted.

Proposition 4. *Let $t(\boldsymbol{u}; \boldsymbol{\rho})$ be the density (5). Then it can be shown that it has the following properties:*

 (i) $t(u_1, u_2, u_3; \rho_{12}, \rho_{13}, \rho_{23}) = t(u_1 + \pi, u_2, u_3; -\rho_{12}, -\rho_{13}, \rho_{23})$
$$= t(u_1, u_2 + \pi, u_3; -\rho_{12}, \rho_{13}, -\rho_{23})$$
$$= t(u_1, u_2, u_3 + \pi; \rho_{12}, -\rho_{13}, -\rho_{23}),$$

 (ii) $t(\boldsymbol{u}; \boldsymbol{\rho}) = -t(\boldsymbol{u}; -\boldsymbol{\rho})$,

 (iii) $t(-\boldsymbol{u}; \boldsymbol{\rho}) = t(\boldsymbol{u}; \boldsymbol{\rho})$.

The property (i) of Proposition 4 implies that changing the signs of two parameters corresponds to the location shift of a variable. Property (ii) shows how crucial the condition $\rho_{12}\rho_{13}\rho_{23} > 0$ (or (9)) actually is as it prevents from negative densities for other parameter combinations. Note that for the alternative expression (12), it holds that $\tilde{t}(\boldsymbol{u}; \boldsymbol{\rho}) = \tilde{t}(\boldsymbol{u}; -\boldsymbol{\rho})$. Finally property (iii) implies that our proposed density is symmetric about its center.

Figure 1 shows the density of TWCC($\boldsymbol{\rho}$) for fixed values of the third component u_3 and selected values of the parameters subject to condition (25), but not generally subject to $\rho_{12}\rho_{13}\rho_{23} = 1$. The figure shows that the TWCC($\boldsymbol{\rho}$) density can have a wide range of dependence structure and strength of dependence. The plots (a)–(d) indicate that the dependence between U_1 and U_2 becomes strong when the parameter $|\rho_{13}|$ is close to $|\rho_{23}|$ or equivalently $|\rho_{23.13}|$ approaches 1. The comparison among the plots (a) and (e)–(g) suggests that the closer value of $|\rho_{12}|$ is to its boundary, namely, $|\rho_{12}| \simeq |\rho_{13}\rho_{23}|/(|\rho_{13}| - |\rho_{23}|) \simeq 0.23$, the greater the concentration of U_1 for fixed values of u_3. Also, it can be seen from plots (a) and (h)–(j) that the values of u_3 control the location of $(u_1, u_2)'$ when the density TWCC($\boldsymbol{\rho}$) given by (5) is viewed as a function of $(u_1, u_2)'$. Finally, as visual confirmation of Theorem 7, the modes and antimodes of TWCC($\boldsymbol{\rho}$) in all the frames are at $u_1 = u_2 = u_3$ and $u_1 + \pi = u_2 = u_3$, respectively.

Additional contour plots of the reparametrized TWCC density with the parameter constraint $\rho_{12}\rho_{13}\rho_{23} = 1$ are provided in Section B in the Appendix. As discussed there, it is advantageous to reparametrize the parameters of the constrained TWCC($\boldsymbol{\rho}$) to those based on ρ_{12} and $\rho_{23.13}$ for a better interpretation of the parameters.

4 Parameter Estimation

In this section we consider methods of moments estimation and maximum likelihood estimation. Throughout this section, let $\{(u_{1m}, u_{2m}, u_{3m})'\}_{m=1}^n$ be a realization of a random sample $\{(U_{1m}, U_{2m}, U_{3m})'\}_{m=1}^n$ from the distribution TWCC($\boldsymbol{\rho}$).

4.1 Method of moments estimation

Method of moments estimators can be obtained by equating theoretical and empirical trigonometric moments

$$E\left\{e^{i(p_1 U_1 + p_2 U_2 + p_3 U_3)}\right\} = \frac{1}{n} \sum_{m=1}^n e^{i(p_1 u_{1m} + p_2 u_{2m} + p_3 u_{3m})}$$

for some selected values of $(p_1, p_2, p_3)' \in \mathbb{Z}^3$. In order to estimate the parameters of the original distribution TWCC($\boldsymbol{\rho}$), possible choices of $(p_1, p_2, p_3)'$ are $(p_i, p_j, p_k)' = (1, -1, 0)'$ with $i < j$. In this case, equation (22) implies that (following lengthy but simple calculations for the second equality)

$$E\left\{e^{i(U_i - U_j)}\right\} = -\rho_{jk}\left(\frac{\varphi_{jk}}{\rho_{ij}} + \frac{1}{\rho_{ik}}\right) = \varphi_{ij}.$$

It follows that the parameters can be estimated as the solution of the following equations:

$$\hat{\varphi}_{ij} = \frac{1}{n} \sum_{m=1}^n e^{i(u_{im} - u_{jm})}, \quad 1 \le i < j \le 3,$$

where $\hat{\varphi}_{ij}$ is the estimate of φ_{ij} defined in (21). Since there is no closed expression for $\{\hat{\rho}_{ij}\}$, numerical derivation of these estimates from $\{\varphi_{ij}\}$ is required. This is convoluted as the $\{\rho_{ij}\}$ do not directly depend on $\{\varphi_{ij}\}$ but through the two equations related to ϕ_{ij}, see (11) and (21). Further, the parameter constraints (8) and (9) have to be satisfied, which makes the method of moments approach a numerically challenging task and we will not pursue it since we could compute the maximum likelihood estimator as described in the section below.

4.2 Maximum likelihood estimation (MLE)

For the original model (5), the likelihood function for $\{\boldsymbol{u}_m\}_{m=1}^n = \{(u_{1m}, u_{2m}, u_{3m})'\}_{m=1}^n$ is given by

$$\log L(\boldsymbol{\rho}) = \log \prod_{m=1}^n t(\boldsymbol{u}_m) = n \log c_2 - \sum_{m=1}^n \log F_m, \tag{27}$$

where $F_m = c_1 + 2\{\rho_{12} \cos(u_{1m} - u_{2m}) + \rho_{13} \cos(u_{1m} - u_{3m}) + \rho_{23} \cos(u_{2m} - u_{3m})\}$. Its score function is

$$\frac{\partial}{\partial \rho_{ij}} \log L(\boldsymbol{\rho}) = n \frac{\frac{\partial c_2}{\partial \rho_{ij}}}{c_2} - \sum_{m=1}^n \frac{\frac{\partial c_1}{\partial \rho_{ij}} + 2\cos(u_{im} - u_{jm})}{F_m}$$

where

$$\frac{\partial c_1}{\partial \rho_{ij}} = \frac{\rho_{ik}}{\rho_{jk}} + \frac{\rho_{jk}}{\rho_{ik}} - \frac{\rho_{jk}\rho_{ik}}{\rho_{ij}^2},$$

$$\frac{\partial c_2}{\partial \rho_{ij}} = \frac{1}{(2\pi)^3} \left\{ \rho_{ij}\left(\left(\frac{\rho_{ik}}{\rho_{jk}}\right)^2 + \left(\frac{\rho_{jk}}{\rho_{ik}}\right)^2\right) - \frac{(\rho_{jk}\rho_{ik})^2}{\rho_{ij}^3} - 2\rho_{ij} \right\} \left((2\pi)^3 c_2\right)^{-1}.$$

The maximum likelihood estimates $\hat{\rho}_{12}, \hat{\rho}_{13}, \hat{\rho}_{23}$ are obtained by equating the score function to zero and numerically solving the system of three equations, see below. For the reader's convenience, we provide in Section C in the Appendix the associated expected Fisher information matrix.

Although the proposed density (5) has a simple and closed form, it is essential to keep the parameter constraints (8) and (9) in mind. The simplified constraint $|\rho_{ij}| + |\rho_{ik}| < |\rho_{ij}|^2 |\rho_{ik}|^2$ can further be turned into

$$|\rho_{ij}| > \frac{1 + \{1 + 4|\rho_{ik}|^3\}^{1/2}}{2|\rho_{ik}|^2}$$

by solving an inequality of the second order. Using the expression

$$\zeta_{ij} = \frac{1 + \{1 + 4|\rho_{ik}|^3\}^{1/2}}{2|\rho_{ik}|^2} \frac{1}{\rho_{ij}}, \quad \zeta_{ij} \in (-1, 0) \cup (0, 1),$$

it is straightforward to see that the parameters of the model (5) can be expressed in terms of ρ_{ik} and ζ_{ij} alone (remember that this holds for one choice of i, j, k). The parameter space of this reparametrized model under the constraint $|\rho_{jk}| < |\rho_{ij}\rho_{ik}|/(|\rho_{ij}| + |\rho_{ik}|)$ and $\rho_{12}\rho_{13}\rho_{23} = 1$ is thus

$$\tilde{\Omega} = \{(\zeta_{ij}, \rho_{ik}); \zeta_{ij} \in (-1, 0) \cup (0, 1), \rho_{ik} \in \mathbb{R} \setminus \{0\}\}.$$

For notational convenience, write $\log L(\rho_{12}, \rho_{13}, \rho_{23}) = \log L(\zeta_{ij}, \rho_{ik})$ if the log-likelihood function (27) is represented in terms of (ζ_{ij}, ρ_{ik}). Then the maximum likelihood estimation for the proposed model can be carried out as follows:

Step 1. For (j, k) successively being equal to $(1, 2), (2, 3), (3, 1)$, obtain the following estimates

$$(\tilde{\zeta}_{ij}, \tilde{\rho}_{ik}) = \underset{(\zeta_{ij}, \rho_{ik}) \in \tilde{\Omega}}{\arg \max} \log L(\zeta_{ij}, \rho_{ik}).$$

Step 2. Among the three obtained maximized quantities, calculate

$$(\hat{\zeta}_{i^*j^*}, \hat{\rho}_{i^*k^*}) = \underset{(\tilde{\zeta}_{ij}, \tilde{\rho}_{ik})}{\arg \max} \log L(\tilde{\zeta}_{ij}, \tilde{\rho}_{ik}).$$

Step 3. Record the maximum likelihood estimate $(\hat{\rho}_{12}, \hat{\rho}_{13}, \hat{\rho}_{23})'$ as

$$\hat{\rho}_{i^*k^*} = \hat{\rho}_{i^*k^*}, \quad \hat{\rho}_{i^*j^*} = \frac{1 + \{1 + 4|\hat{\rho}_{i^*k^*}|^3\}^{1/2}}{2|\hat{\rho}_{i^*k^*}|^2} \frac{1}{\hat{\zeta}_{i^*j^*}}, \quad \hat{\rho}_{j^*k^*} = \frac{1}{\hat{\rho}_{i^*j^*}\hat{\rho}_{i^*k^*}},$$

where $i^* \neq j^* \neq k^*$.

The algorithm is repeated with different initial values, to make sure that the global maximum is achieved. The initial values for the parameters ζ_{ij} and ρ_{ik} are uniformly chosen from the intervals they are allowed to take values in (where of course the infinite intervals for ρ_{ik} are limited to a large maximal value). The function for calculating the ML estimates was written in the programming language R, using the optimizer solnp from the library Rsolnp [16] and is available in the GitHub repository `https://github.com/Sophia-Loizidou/Trivariate-wrapped-Cauchy-copula`. The consistency of this approach is shown and its finite-sample performance is investigated by means of Monte Carlo simulations, which we provide in Section D in the Appendix.

5   Adding specified angular and/or linear marginals to the TWC copula

Let $(U_1, U_2, U_3)'$ be a random vector which follows the TWCC($\boldsymbol{\rho}$). Assume that either

  - f_i is a density on the circle $[0, 2\pi)$ $(i = 1, 2, 3)$ and F_i its distribution function with fixed and arbitrary origin, namely, $F_i(\theta) = \int_{c_i}^{\theta} f_i(x)dx$ with $c_i \in [0, 2\pi)$;
  - f_i is a density on (a subset of) the real line $\mathbb{R}$ $(i = 1, 2, 3)$ and F_i its distribution function.

Define

$$(\Theta_1, \Theta_2, \Theta_3)' = \left(F_1^{-1}\left(\frac{U_1}{2\pi}\right), F_2^{-1}\left(\frac{U_2}{2\pi}\right), F_3^{-1}\left(\frac{U_3}{2\pi}\right) \right)'.$$

Then it follows that $(\Theta_1, \Theta_2, \Theta_3)'$ has the joint density

$$f(\boldsymbol{\theta}; \boldsymbol{\rho}) = (2\pi)^3 c_2 \left(c_1 + 2 \sum_{1 \leq i < j \leq 3} \rho_{ij} \cos[2\pi\{F_i(\theta_i) - F_j(\theta_j)\}] \right)^{-1} \prod_{1 \leq k \leq 3} f_k(\theta_k), \tag{28}$$

where $\boldsymbol{\theta} = (\theta_1, \theta_2, \theta_3)'$ and each θ_i either belongs to $[0, 2\pi)$ or to (a subset of) $\mathbb{R}$. We refer to this extension of TWCC($\boldsymbol{\rho}$) with specified marginals as the extended TWCC. As is clear from the definition, the univariate marginal density of Θ_i is given by f_i $(i = 1, 2, 3)$. This yields a very flexible class of distributions with either

  • 3 angular components,

- 2 angular and 1 linear components,
- 1 angular and 2 linear components,
- or even 3 linear components.

The reason why there is no distinction between the type of marginals lies in the simple fact that the uniform distribution on $[0, 2\pi)$ bears by nature a double role as being linear as well as circular (since all points, and in particular the endpoints, share the same value). This unified viewpoint was not taken up by the two papers [25] and [60], nor in [26] where the concept of copulas for circular data has been discussed in general.

From the properties of $\text{TWCC}(\boldsymbol{\rho})$, we can derive the following general results (whose proof is omitted) for the extended TWCC.

Theorem 8. *Let $(\Theta_1, \Theta_2, \Theta_3)'$ follow the extended TWCC with density (28). Then the following hold for $(\theta_1, \theta_2, \theta_3)'$ each either belonging to $[0, 2\pi)$ or to (a subset of) $\mathbb{R}$:*

(i) *The univariate marginal distribution of Θ_i is $f_i(\theta_i)$.*

(ii) *The bivariate marginal distribution of $(\Theta_i, \Theta_j)'$ is*

$$f(\theta_i, \theta_j) = 4\pi^2 t_2(2\pi F_i(\theta_i), 2\pi F_j(\theta_j); \phi_{ij}) f_i(\theta_i) f_j(\theta_j),$$

where $t_2(\cdot, \cdot)$ is the density (10).

(iii) *The bivariate conditional distribution of $(\Theta_i, \Theta_j)'$ given $\Theta_k = \theta_k$ is*

$$f(\theta_i, \theta_j | \theta_k) = 4\pi^2 t_{2|1}(2\pi F_i(\theta_i), 2\pi F_j(\theta_j) | 2\pi F_k(\theta_k); \boldsymbol{\rho}) f_i(\theta_i) f_j(\theta_j),$$

where $t_{2|1}(\cdot, \cdot | \cdot)$ is the density (15).

(iv) *The univariate conditional distribution of Θ_i given $\Theta_j = \theta_j$ is*

$$f(\theta_i | \theta_j) = 2\pi t_{1|1}(2\pi F_i(\theta_i) | 2\pi F_j(\theta_j); \phi_{ij}) f_i(\theta_i),$$

where $t_{1|1}(\cdot | \cdot)$ is the density (17).

(v) *The univariate conditional distribution of Θ_i given $(\Theta_j, \Theta_k)' = (\theta_j, \theta_k)'$ is*

$$f(\theta_i | \theta_j, \theta_k) = 2\pi t_{1|2}(2\pi F_i(\theta_i) | 2\pi F_j(\theta_j), 2\pi F_k(\theta_k); \delta_{i|jk}) f_i(\theta_i),$$

where $t_{1|2}(\cdot | \cdot, \cdot)$ is the density (18).

These results demonstrate that with our new model all forms of regression analysis involving up to three angular and/or linear components are straightforward, which in a unified way covers what we described as our objective in Section 1. Random number generation from the extended TWCC is also immediate by adding just the step

$$\Theta_i = F_i^{-1}\left(\frac{U_i}{2\pi}\right), \ i = 1, 2, 3,$$

to the algorithm presented in Section 3.2.

The parameters of the extended TWCC as in (28) are estimated using MLE. When the marginals are uniform, the procedure from Section 4.2 applies. In the case that the marginal distributions are not uniform, the maximum likelihood estimates of the parameters are calculated in a two-step approach. Let $\{(\theta_{1m}, \theta_{2m}, \theta_{3m})'\}_{m=1}^{n}$ denote the sequence of toroidal observations from (28). In the first step, the ML estimates of the parameters of the marginals are calculated, followed in the second step by estimating the parameters of the copula using $\{(u_{1m}, u_{2m}, u_{3m})'\}_{m=1}^{n}$ for

$$(u_{1m}, u_{2m}, u_{3m})' = \left(2\pi F_1(\theta_{1m}; \hat{\vartheta}_1), 2\pi F_2(\theta_{2m}; \hat{\vartheta}_2), 2\pi F_3(\theta_{3m}; \hat{\vartheta}_3)\right)',$$

where, for $i \in \{1, 2, 3\}$, F_i represents the marginal density function of θ_i and $\hat{\vartheta}_i$ the parameters obtained from the first step of the maximization. Joe [22] refers to this as the method of inference functions for margins or IFM method. Efficiency and consistency of the estimates obtained with IFM compared to the estimates that can be obtained by performing one maximisation of the likelihood function can be found in Chapter 10 of [22] and Chapter 5 of [23].

We conclude this section by briefly discussing one particular choice of univariate marginals as in Theorem 8(i), namely when each f_i is the wrapped Cauchy density

$$f_i(\theta) = \frac{1}{2\pi} \frac{1 - \xi_i^2}{1 + \xi_i^2 - 2\xi_i \cos(\theta - \mu_i)}, \quad 0 \le \theta < 2\pi, \tag{29}$$

where μ_i is the location parameter and $\xi_i \in (-1, 1)$ the concentration parameter. Assume that the origin of the distribution function F_i is $c_i = \mu_i$. In this case F_i has the closed-form expression

$$F_i(\theta_i) = \frac{1}{\pi} \arctan\left(\frac{1+\xi_i}{1-\xi_i} \tan \frac{\theta_i - \mu_i}{2}\right) + I(\theta_i > \mu_i + \pi), \quad \mu_i < \theta_i < \mu_i + 2\pi.$$

Then, noting that $\cos(2\arctan x) = (1 - x^2)/(1 + x^2)$ and $\sin(2\arctan x) = 2x/(1 + x^2)$, $x \in \mathbb{R}$, it can be shown that the density of (28) can be expressed as

$$f(\boldsymbol{\theta}; \boldsymbol{\rho}) = c_2 \prod_{i=1}^{3}(1 - \xi_i^2)\left[c_1 \prod_{i=1}^{3} g_i(\theta_i) + 2 \sum_{\substack{1 \le j < k \le 3 \\ i \ne j,k}} \rho_{ij} g_k(\theta_k) h_{ij}(\theta_i, \theta_j)\right]^{-1}, \tag{30}$$

where $g_i(\theta_i) = 1 + \xi_i^2 - 2\xi_i \cos(\theta_i - \mu_i)$ and

$$h_{ij}(\theta_i, \theta_j) = (1 + \xi_i^2)(1 + \xi_j^2)\cos(\theta_i - \mu_i)\cos(\theta_j - \mu_j) + (1 - \xi_i^2)(1 - \xi_j^2)\sin(\theta_i - \mu_i)\sin(\theta_j - \mu_j)$$
$$- 2\xi_j(1 + \xi_i^2)\cos(\theta_i - \mu_i) - 2\xi_i(1 + \xi_j^2)\cos(\theta_j - \mu_j) + 4\xi_i\xi_j.$$

Note that the density (30) does not involve any integrals. As further nice properties derived from Theorem 8, the wrapped Cauchy copula with wrapped Cauchy marginals also has wrapped Cauchy conditionals for Θ_i given $\Theta_j = \theta_j$ and for Θ_i given $(\Theta_j, \Theta_k)' = (\theta_j, \theta_k)'$. Moreover, the bivariate marginal distribution of $(\Theta_i, \Theta_j)'$ is the bivariate wrapped Cauchy distribution of [31] with density

$$f(\theta_i, \theta_j) = \tilde{\gamma}\left\{\tilde{\gamma}_0 - \tilde{\gamma}_1 \cos(\theta_i - \mu_i) - \tilde{\gamma}_2 \cos(\theta_j - \mu_j) - \tilde{\gamma}_3 \cos(\theta_i - \mu_i)\cos(\theta_j - \mu_j)\right.$$
$$\left. - \tilde{\gamma}_4 \sin(\theta_i - \mu_i)\sin(\theta_j - \mu_j)\right\}^{-1},$$

where $\tilde{\gamma} = (1 - \rho_{ij}^2)(1 - \xi_i^2)(1 - \xi_j^2)/(4\pi^2)$, $\tilde{\gamma}_0 = (1 + \rho_{ij}^2)(1 + \xi_i^2)(1 + \xi_j^2) - 8\rho_{ij}\xi_i\xi_j$, $\tilde{\gamma}_1 = 2(1 + \rho_{ij}^2)\xi_i(1 + \xi_j^2) - 4\rho_{ij}(1 + \xi_i^2)\xi_j$, $\tilde{\gamma}_2 = 2(1 + \rho_{ij}^2)(1 + \xi_i^2)\xi_j - 4\rho_{ij}\xi_i(1 + \xi_j^2)$, $\tilde{\gamma}_3 = -4(1 + \rho_{ij}^2)\xi_i\xi_j + 2\rho_{ij}(1 + \xi_i^2)(1 + \xi_j^2)$, and $\tilde{\gamma}_4 = 2\rho_{ij}(1 - \xi_i^2)(1 - \xi_j^2)$. Random number generation from the distribution (30) can be carried out using the Möbius transformation

$$\Theta_i = F_i^{-1}\left(\frac{U_i}{2\pi}\right) = \mu_i + 2\arctan\left[\frac{1 - \xi_i}{1 + \xi_i}\tan\left(\frac{U_i}{2}\right)\right].$$

6 Comparison with existing models from the literature

Having discussed the main properties of our new copula, we can now proceed to a comparison with respect to the competitors from the literature. This is the first paper on trivariate copulas for both angular and cylindrical data so there is no direct competitor.

A d-dimensional toroidal copula model has been proposed in [33] by directly extending the copula construction (2) to

$$f(\theta_1, \theta_2, \ldots, \theta_d) = (2\pi)^m \prod_{j=1}^{m}\left\{g\left[2\pi \sum_{i=j}^{d} F_i(\theta_i)\right]\right\} \prod_{i=1}^{d} f_i(\theta_i)$$

where $1 \le m \le d - 1$ and the f_i and F_i, $i = 1, \ldots, d$, are respectively circular density and distribution functions. Their suggested three-dimensional copula corresponds to $d = 3$ and $m = 1$. The authors investigate various inferential properties and show that the conditional distributions are of the same form as the general copula. In contrast to our model, their model lacks symmetry concerning the permutation of variables when $m > 1$; specifically, $f(\theta_i, \theta_j, \theta_k)$ and $f(\theta_k, \theta_i, \theta_j)$ represent essentially different models. Further properties such as moments, modality, identifiability, bivariate marginal distributions, random number generation, ease of parameter estimation, parameter interpretability are not discussed and hence difficult to evaluate. The authors also do not provide suggestions as to which combinations of marginals and copula g are viable.

Further, a real data comparison given in their paper shows that, in terms of AIC, a better model is the multivariate nonnegative trigonometric sums (MNNTS) model of [9] for a trivariate angular protein data. The probability density function of the MNNTS is given by

$$f(\theta_1, \theta_2, \ldots, \theta_d) = \sum_{k_1=0}^{M_1}\sum_{k_2=0}^{M_2}\cdots\sum_{k_d=0}^{M_d}\sum_{m_1=0}^{M_1}\sum_{m_2=0}^{M_2}\cdots\sum_{m_d=0}^{M_d} c_{k_1 k_2 \cdots k_d}\bar{c}_{m_1 m_2 \cdots m_d} e^{\sum_{s=1}^{d} \mathrm{i}(k_s - m_s)\theta_s} \tag{31}$$

13

where $c_{k_1 k_2 \cdots k_d}, \bar{c}_{m_1 m_2 \cdots m_d}$ are the parameters and $\bar{c}$ is the complex conjugate of c.

The paper [33] also considers the well-established multivariate von Mises distribution of [44] which again does not do as well for that dataset though this model belongs to the exponential family so inherits several desirable properties of this family.

There are other choices such as the multivariate Generalised von Mises (mGvM) distribution ([51]), the multivariate wrapped normal distribution ([3]), the multivariate projected normal distribution ([49]), and the inverse stereographic normal distribution ([54]), but these all have some limitations in comparison to our model such as either their normalizing constants are intractable so the MLE computations are not easy, they may be multimodal, or sampling is not clear-cut. Hence, we have selected only the MNNTS as competitor in Section 7.1 for our protein data.

7 Practical applications

7.1 Protein data

Predicting the 3D structure of proteins is a cutting-edge area of research in bioinformatics and computational biology. Mardia [42] has provided a recent overview on statistical approaches to three major areas in protein structural bioinformatics and listed the main challenges lying ahead. As mentioned in Section 1, an essential challenge is the ability to jointly model the conformational angles ϕ, ψ (dihedral angles) and ω (torsion angle of the side chain). Indeed, the recent Nature Methods paper [35] emphasises "distributions of conformations are the future of structural biology". The main body of statistical research in this direction has so far concentrated on the two conformational angles ϕ, ψ, which has already led to important contributions in the protein structure prediction problem, see for example [5], [19], [12], [18], and Chapters 1 and 4 of [38]. This is due to the fact that, theoretically, the torsion angle ω is either 0 or 180 degrees, corresponding to peptide planarity. However, [4] have investigated this issue in detail and shown that peptide planarity is not a common feature for collected data. In their paper, they conduct an exploratory data analysis of all three conformational angles. The authors from [48], [44] and [33] have modelled three or more angles with their proposed distributions. The main problem of statistical approaches to protein structure prediction is that they are computationally intensive (especially due to intricate normalizing constants), and we believe that our proposal, which is a faster method, can make the statistical approach more feasible.

We now give some background to protein structure. The building blocks of proteins are the amino acids, which consist of the backbone and the sidechains. The backbone consists of the chemical bonds NH-Cα and Cα-CO, where Cα denotes the central Carbon atom. These bonds can rotate around their axes, with ϕ denoting the NH-Cα angle and ψ the Cα-CO angle. These angles need to be studied as specific combinations of them allow the favourable hydrogen bonding patterns, while others can 'result in clashes within the backbone or between adjacent sidechains' [20, 42, 43]. The ω angle denotes the N-C torsion angle, where C is the non-central carbon atom. As we have said before, theoretically the angle ω can only take the values 0 and π, and in some of the research work, this angle was fixed at one of the two values [2, 19]. However, in practice this angle is often measured with some noise and using our extended TWCC, we shall model all three angles. In bioinformatics, all three angles are studied in [4] and we will give some comments on how their exploratory work is explained by our model.

For the present data analysis, we consider position 55 at 2000 randomly selected times in the molecular dynamic trajectory of the SARS-CoV-2 spike domain from [15]. The position occurs in α-helix throughout the trajectory. DPPS [28] is used to compute the secondary structure and [6] to verify the chains. As can be seen from Figure 2, the marginal distributions of the angles ϕ, ψ and ω for this dataset cannot be modelled by the uniform distribution on the circle, so other distributions need to be explored. Conveniently, our trivariate wrapped Cauchy copula allows us to choose different marginals, which is why we combined it respectively with wrapped Cauchy, cardioid, von Mises and Kato–Jones marginals. Of course, many other choices are possible, and one can also combine distinct marginals. Whatever marginals we choose, the parameters of our models are estimated using MLE as explained in Section 5 and a model comparison is carried out using the Akaike Information Criterion (AIC) and the Bayesian Information Criterion (BIC). Alternatively, it is also viable to estimate the marginals in a non-parametric way and then combine the estimated marginals with our copula (see [14] for such a procedure in $\mathbb{R}^d$).

As plotting all three angles at the same time is not possible, Figure 4 shows the plots of the data of two of the angles given the third one. The values of the fixed angles in radians ($\phi = 1.93$, $\psi = 2.8$ and $\omega = 0$) are chosen to be the mode of the data, and only points that are within 0.1 radians of the selected value of the fixed angle are plotted. In order to make the plots clearer, the range of values on each axis is not between 0 and 2π, like the traditional Ramachandran plot, but it is chosen such that both the contour plots and the points are visible (in summary, we have re-scaled the plots). For the values of ω, most observations were around 0 and so the plot is translated from $[0, 2\pi)$ to $[-\pi, \pi)$ such that making the range of values on the axis smaller is possible. The contour plots correspond to our copula density (5) with the
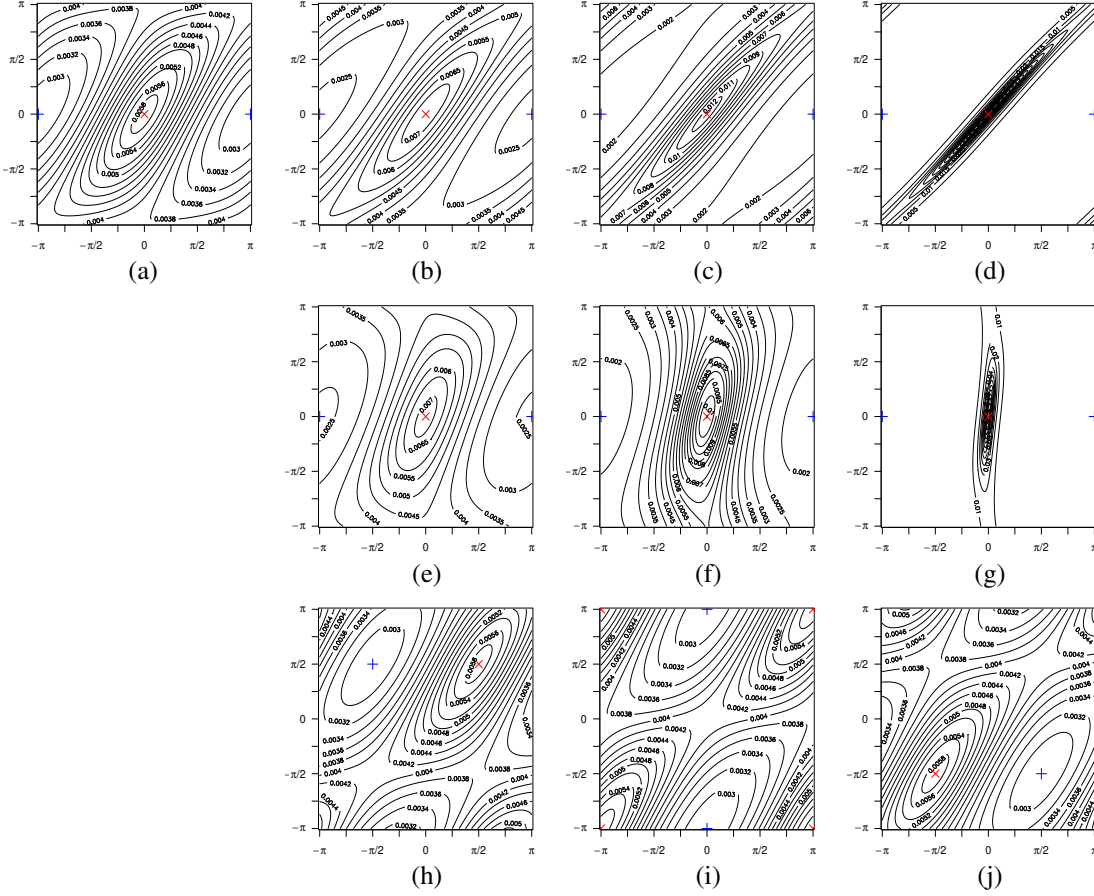
14

Figure 1: Contour plots of the density of TWCC(ρ) with $\rho_{23} = 0.2$ and: (a)–(d) $(-\rho_{12}, u_3) = (2.5, 0)$ and (a) $-\rho_{13} = 2$, (b) $-\rho_{13} = 1$ and (c) $-\rho_{13} = 0.5$ and (d) $-\rho_{13} = 0.25$, (e)–(g) $(-\rho_{13}, u_3) = (2, 0)$ and (e) $-\rho_{12} = 1$, (f) $-\rho_{12} = 0.5$ and (g) $-\rho_{12} = 0.25$, and (h)–(j) $(-\rho_{12}, -\rho_{13}) = (2.5, 2)$ and (h) $u_3 = \pi/2$, (i) $u_3 = \pi$ and (j) $u_3 = 3\pi/2$. The x-axis represents the value of u_1, while the y-axis denotes the value of u_2. The symbols '$\times$' (red) and '+' (blue) denote the modes and antimodes of density (5), respectively.
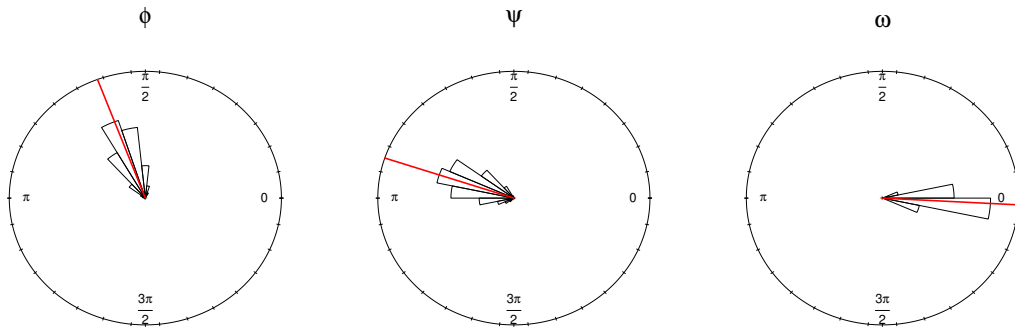
Figure 2: Rose plots of the protein data. The marginals are not uniformly distributed on the circle. The mean direction as calculated using von Mises marginal densities is plotted in red.

15

marginal distributions being the von Mises distribution, whose density is given by

$$f(\theta) = \frac{1}{2\pi I_0(\kappa)} \exp^{\kappa \cos(\theta - \mu)}, \quad \theta \in [0, 2\pi), \tag{32}$$

where $I_0(\kappa)$ denotes the modified Bessel function of the first kind and order 0. The von Mises marginals with their lighter tails lead to the best fit for this concentrated dataset, as measured by both AIC and BIC, see Table 1. The observed data points are plotted on top of the contours. This gives a visual indication of how good our estimated model fits this protein dataset. For the extended TWCC with von Mises marginals, the standard errors of the estimated parameters can be evaluated by means of bootstrap. Using $B = 1000$ bootstrap samples, the maximum likelihood estimates of the parameters, with the standard error given in parenthesis, are $\hat{\rho}_{12} = 9.18(4.99), \hat{\rho}_{13} = -1.17(4.60), \hat{\rho}_{23} = -0.09(4.41)$ for the copula parameters and $\hat{\mu}_1 = 1.93(0.0043), \hat{\kappa}_1 = 27.6(0.99), \hat{\mu}_2 = 2.82(0.0055), \hat{\kappa}_2 = 17.3(0.62), \hat{\mu}_3 = 6.23(0.0024), \hat{\kappa}_3 = 84.4(2.95)$, where $\hat{\mu}_i$ and $\hat{\kappa}_i$ denote the estimated values for μ and κ of density (32) corresponding to the marginal distribution of θ_i for $i \in \{1, 2, 3\}$. We attribute the relatively high standard errors of the copula parameters to the condition (9) which links all three parameters.

The estimate of a modified partial dependence parameter $\rho^*_{23.13}(\equiv \rho_{23}/|\rho_{13}|)$ is $\hat{\rho}^*_{23.13} = -0.0769$, while the estimate of the full dependence parameter $\rho^*_{12}(\equiv (1 - |\rho^*_{23.13}|)^{3/2}/|\rho^*_{23.13}|^{1/3}\rho_{12})$ is $\hat{\rho}^*_{12} = 20.5$. As discussed in Section B in the Appendix, $\rho^*_{23.13}$ measures the strength of dependence between u_1 and u_2 for large $|\rho_{12}|$, considering its absolute value, and inherits the same sign as ρ_{23}. The full dependence parameter ρ^*_{12} is a reparameterization of ρ_{12}, which simplifies the parameter range to $|\rho^*_{12}| \geq 1$ and retains the original sign of ρ_{12}.

Since $|\hat{\rho}^*_{12}|$ is large, it follows from Proposition 3(ii) that the estimated density of TWCC($\hat{\rho}$) can be approximated by the limiting copula density (26). This can be confirmed in Figure 3(a) and (b), which show the estimated density of TWCC($\hat{\rho}$) and the limiting density (26) for a fixed value of u_3, respectively. Hence the estimated density of TWCC($\hat{\rho}$) has a shape similar to (26), which has a linear dependence structure between u_1 and u_2 for a fixed u_3. On the other hand, as can be seen in Figure 3(c), the dependence structure between u_1 and u_3 for a fixed u_2 is far from a linear relationship. Indeed, we have $(\hat{\rho}^*_{23.12}, \hat{\rho}^*_{13})' = (-0.00980, -5.43)'$, and it seems that $|\rho^*_{13}|$ is not large enough compared with the value of $|\hat{\rho}^*_{23.12}|$ to validate the assumption on the limiting density (26); see Figure 1. Also, as can be seen in Figure 3(d), the relationship between u_2 and u_3 for a fixed u_1 is different from the linear dependence structure.

Our findings regarding the angle ω confirm the exploratory analysis done by [4]: the data points are strongly concentrated around the modal direction $\hat{\mu}_3$, but are not exactly equal to that value, as can also be visually appreciated from the plot in Figure 2. The inherent tractability of our model allows biologists and bioinformaticians to quantify uncertainties, compute quantities of interest, and in particular our straightforward random number generation process enables them to quickly simulate data from our model, which is essential in their pipelines [59].

We conclude this section by a comparison of our model with the MNNTS distribution (31) of [9] which we summarized in Section 6. Table 1 presents the fit of various models. The maximised log-likelihood, AIC and BIC are reported for each model, along with the number of free parameters, denoted by p. The algorithms for fitting the MNNTS distribution are taken from the R package CircNNTS [10]. Besides the reasons mentioned in Section 6 to compare our model to the MNNTS, it is also the only competitor for which we could find implemented and working code. The number of free parameters for MNNTS(M_1, M_2, M_3) is calculated as $2\left(\prod_{i=1}^{3}(M_i + 1) - 1\right)$. Various combinations of the values M_1, M_2, M_3 are shown in Table 1, with the number of free parameters increasing rapidly. The MNNTS is not able to match the fit of our copula (not only in terms of AIC/BIC but even in terms of log-likelihood), even for a very large number of parameters. The best model for all three measures of fit, the trivariate wrapped Cauchy copula with von Mises marginals, is shown in bold.

7.2 Climate data

For the second real data application, we use a time series of 1326 observations of red half-hourly wave directions and heights, recorded in the period 15/02/2010 – 16/03/2010 by the buoy of Ancona, located in the Adriatic Sea at about 30 km from the coast. The data points are collected far spaced enough from each other to be considered independent. In order to address the climate-change related problem of modelling wave data mentioned in Section 1 and to get a more complete picture than just wave height (linear, x) and direction (circular, θ_1), we also add the wind direction (circular, θ_2). The data thus is on a hyper-cylinder, which we can analyze with our copula. We choose as our circular marginals the wrapped Cauchy distribution and the Weibull distribution for the linear marginal. Of course, many other combinations could be considered, but these work as we see. Due to the multimodality of the data, a mixture model is required, so we use densities of the form

$$f(\theta_1, \theta_2, x) = \sum_{i=1}^{K} \pi_i f_i(\theta_1, \theta_2, x), \quad \sum_{i=1}^{K} \pi_i = 1, \tag{33}$$

16

Table 1: Maximized log-likelihood, AIC, BIC, and the number of free parameters (denoted by p) for the two models (extended TWCC and MNNTS) for the protein dataset.

Model	Marginals	log-likelihood	AIC	BIC	p
	uniform	-7920	15845	15862	2
	wrapped Cauchy	1131	-2245	-2194	8
Extended TWCC	cardioid	-3495	7007	7058	8
	von Mises	**2046**	**-4074**	**-4023**	**8**
	Kato–Jones	1404	-2778	-2694	14
	(M_1, M_2, M_3)				
	(0,0,0)	-11027	22055	22055	0
	(1,1,1)	-6923	13874	13953	14
	(2,2,2)	-4582	9268	9559	52
	(3,3,3)	-2984	6220	6926	126
MNNTS	(4,4,4)	-1811	4118	5507	248
	(5,5,5)	-921	2702	5111	430
	(6,6,6)	-231	1829	5660	684
	(7,7,7)	315	1414	7138	1022
	(8,8,8)	746	1421	9575	1456
	(9,9,9)	1091	1815	13005	1998
	(10,10,10)	1370	2579	17478	2660

where K is the number of components of the mixture model, π_i is the weight of each class $i = 1, \ldots, K$ and $f_i(\theta_1, \theta_2, x)$ is the density of component i and is the copula as defined in (28), with marginals as already explained. In order to estimate the parameters, we use a variant of the Expectation-Maximization (EM) algorithm to find the values of the parameters for each component of the mixture model. As with maximum likelihood estimation with non-uniform marginals, the maximisation is done as a first step for the parameters of the marginal distributions and then, using the obtained parameters, estimates of the parameters of the copula are obtained. The M-step of our algorithm thus adopts the IFM method described in Section 5, which is why we speak of a variant of the EM algorithm, which for the rest works exactly like an EM algorithm. The initial values for the parameters were randomly chosen. This was repeated 10 times and the parameters that maximised the log-likelihood were chosen. To find the number of mixture components, we considered the values $K = 2, 3, 4, 5$ and used the BIC to determine the best-fitting model.

We found that $K = 4$ components fit best the data, as the BIC values are 16045, 15850, 10750 and 15655, for $K = 2, 3, 4, 5$, respectively. The parameter estimates for this mixture model are given in Table 2. It should be noted that in each of the clusters, one of the ρ_{ij} is large in absolute value, meaning that we are in the limit case given by density (26). The values of the ρ_{ij}s are very different between each cluster, with Cluster 3 having a very large negative value for $\hat{\rho}_{12}$, Cluster 1 having a smaller negative value for the same parameter and Cluster 2 having a large positive value for $\hat{\rho}_{13}$. The values of the parameters calculated for Cluster 4 are not as extreme. For visualization of the results, the bivariate marginal distribution is plotted in Figure 5, as given in Theorem 8, with N, E, S, W representing north, east, south and west, respectively. The plots on the left hand side are scatter plots of the data, coloured according to their cluster as given by our variant of the EM algorithm with 4 components. The same colour is used for each cluster to plot the bivariate marginal distribution for each of the components. In the Adriatic sea, the predominant winds are bora, coming from north/north-east, and sirocco, from the south-east. The different winds are captured in different clusters of the data, with the red and green cluster being caused by the bora wind and dark blue by the sirocco wind.

8 Discussion

In this paper we have proposed a new distribution on the three-dimensional torus, the trivariate wrapped Cauchy copula. The marginal and conditional distributions of the copula are known distributions and random variate generation is simple and efficient through a transformation of uniform random variates without rejection. The proposed distribution is unimodal for any value of the parameters ρ_{12}, ρ_{13} and ρ_{23}, a very important and rare property in hypertoroidal distributions. Parameter estimation can be performed via maximum likelihood estimation. As the distribution is a copula, the marginal distributions of the components can be chosen as any univariate angular or linear distributions. As illustrated in our protein data example, an attractiveness of our flexible model is that the choice of marginals allows us to model more or less concentrated data. Choosing marginal distributions that are defined on the real line allows the copula to also model data that do not have all three components as angular variables. This was done for the second example, where mixture models were fitted to data that include one linear and two angular variables.
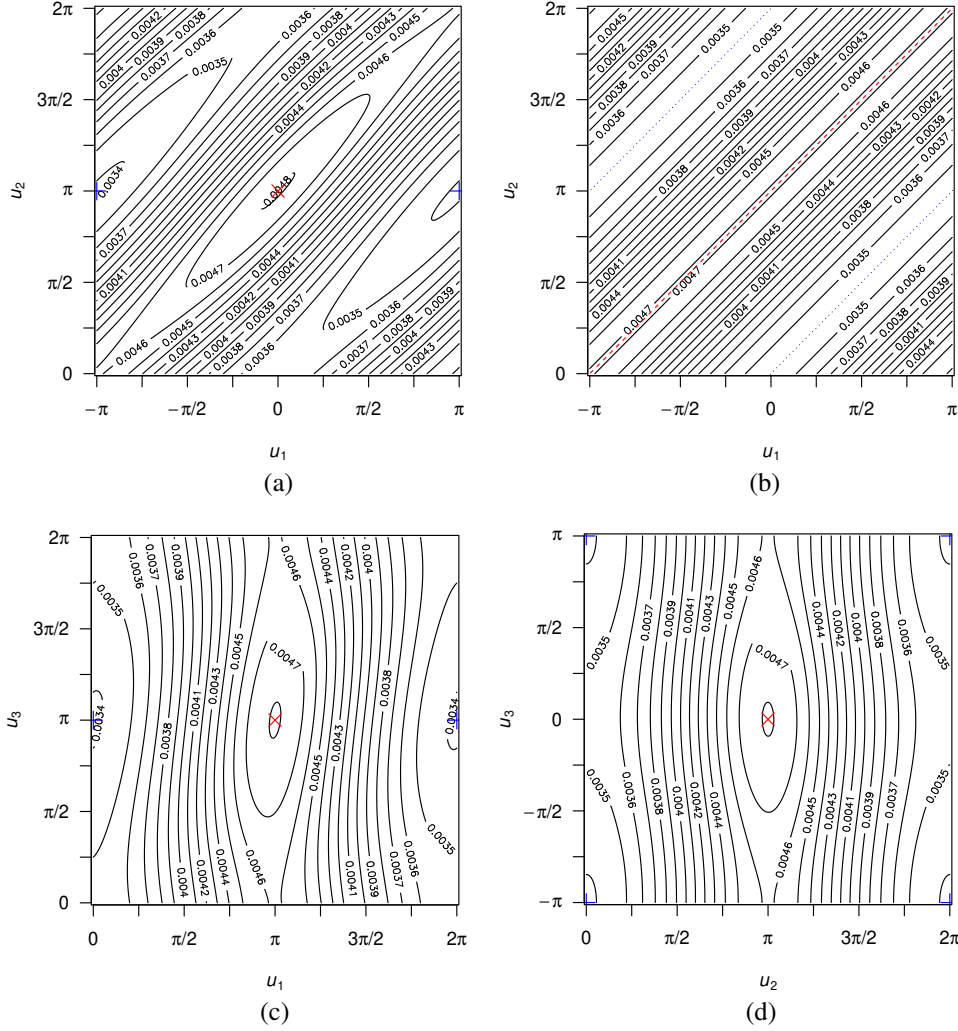
Figure 3: Contour plots of: the estimated density of TWCC($\hat{\boldsymbol{\rho}}$) as a function of (a) $(u_1, u_2)'$, (c) $(u_1, u_3)'$, and (d) $(u_2, u_3)'$ with the other variable fixed at 0, and (b) the limiting copula density $t(u; \hat{\boldsymbol{\rho}})$ given in (26) as a function of $(u_1, u_2)'$ with $u_3 = 0$, where $\hat{\boldsymbol{\rho}} = (9.18, -1.17, -0.09)'$. The symbol '$\times$' or a dashed line (both in red) denote the mode(s) of the density, while '+' or dotted lines (both in blue) denote the antimode(s) of the density.

Table 2: Parameter estimates as obtained from our variant of the EM algorithm for 4 components. The marginal distributions for wind and wave directions are wrapped Cauchy, and the estimates of the parameters are denoted by $\hat{\rho}_1, \hat{\mu}_1$ and $\hat{\rho}_2, \hat{\mu}_2$, respectively, with π representing north. For the wave height we use the Weibull distribution, where $\hat{\lambda}_3$ is the estimated scale parameter and $\hat{\nu}_3$ the estimated shape parameter. Finally $\hat{\pi}_i$ denotes the estimate of the weight of class i.

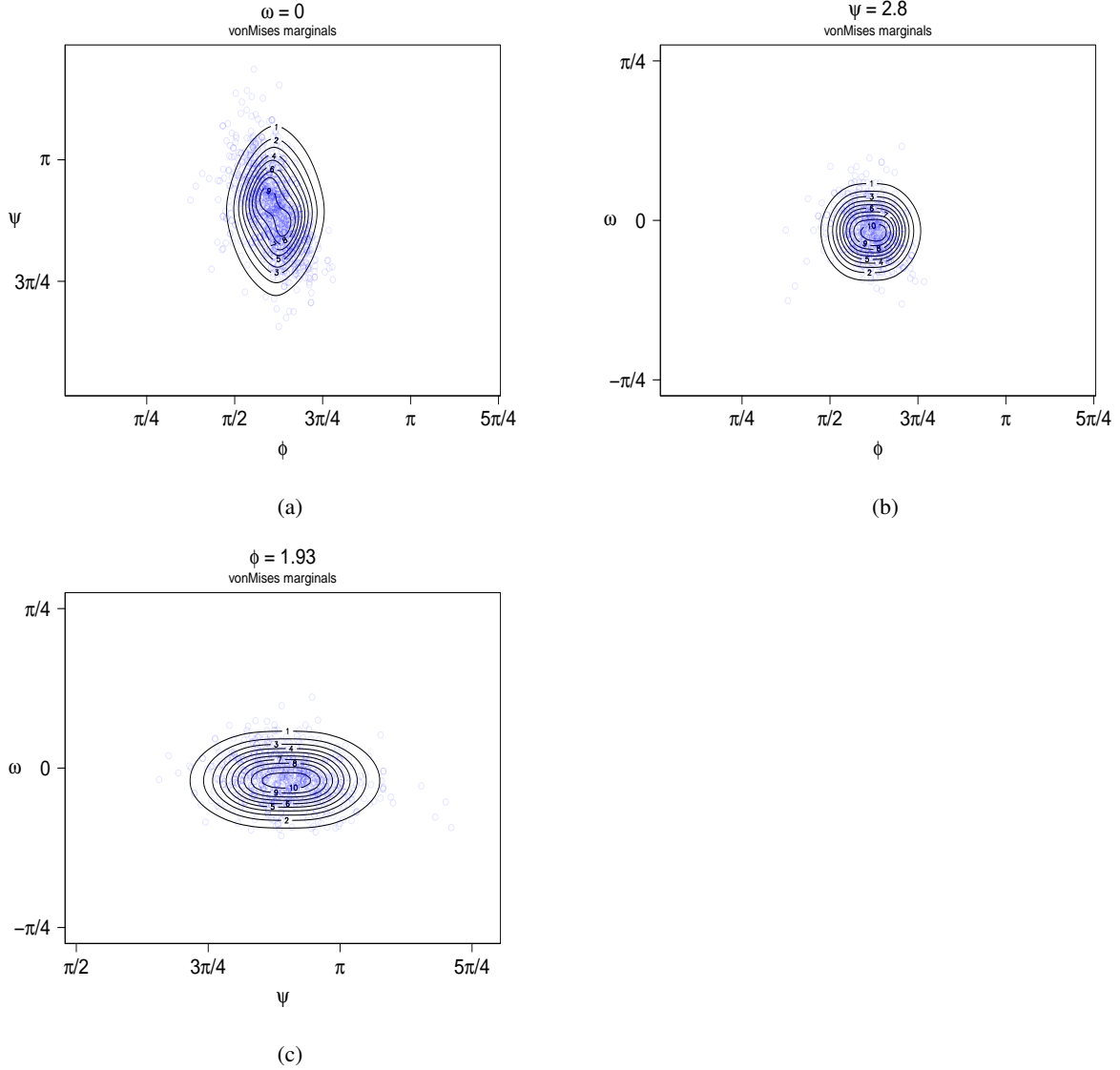| Parameters	Cluster 1	Cluster 2	Cluster 3	Cluster 4
$\hat{\rho}_{12}$	-92.092	-0.008	-5956.914	-5.168
$\hat{\rho}_{13}$	43.331	584.384	-0.032	0.864
$\hat{\rho}_{23}$	-0.0003	-0.218	0.005	-0.224
$\hat{\mu}_1$	3.869	4.440	5.184	2.588
$\hat{\rho}_1$	0.834	0.882	0.809	0.578
$\hat{\mu}_2$	3.772	4.460	5.692	2.239
$\hat{\rho}_2$	0.729	0.887	0.432	0.736
$\hat{\lambda}_3$	1.781	3.414	0.948	0.766
$\hat{\nu}_3$	3.207	3.390	1.531	1.424
$\hat{\pi}_i$	0.184	0.054	0.546	0.216

Figure 4: Contour plots of density (5) with von Mises marginals, with parameter values estimated by maximum likelihood. The parameters of the marginals are $\hat{\mu}_1 = 1.93, \hat{\kappa}_1 = 27.6, \hat{\mu}_2 = 2.82, \hat{\kappa}_2 = 17.3, \hat{\mu}_3 = 6.23, \hat{\kappa}_3 = 84.4$, where $\hat{\mu}_i$ and $\hat{\kappa}_i$ denote the estimated value for μ and κ of density (32) corresponding to the marginal distribution of θ_i for $i \in \{1, 2, 3\}$, and the copula parameters are $\hat{\rho}_{12} = 9.18, \hat{\rho}_{13} = -1.17, \hat{\rho}_{12} = -0.09$. The values of the fixed angles (shown in each title) are chosen to be the mode of the data, and only points that are within 0.1 radians of the chosen value of the fixed angle are plotted. For illustration purposes, the three plots are portrayed on different scales.
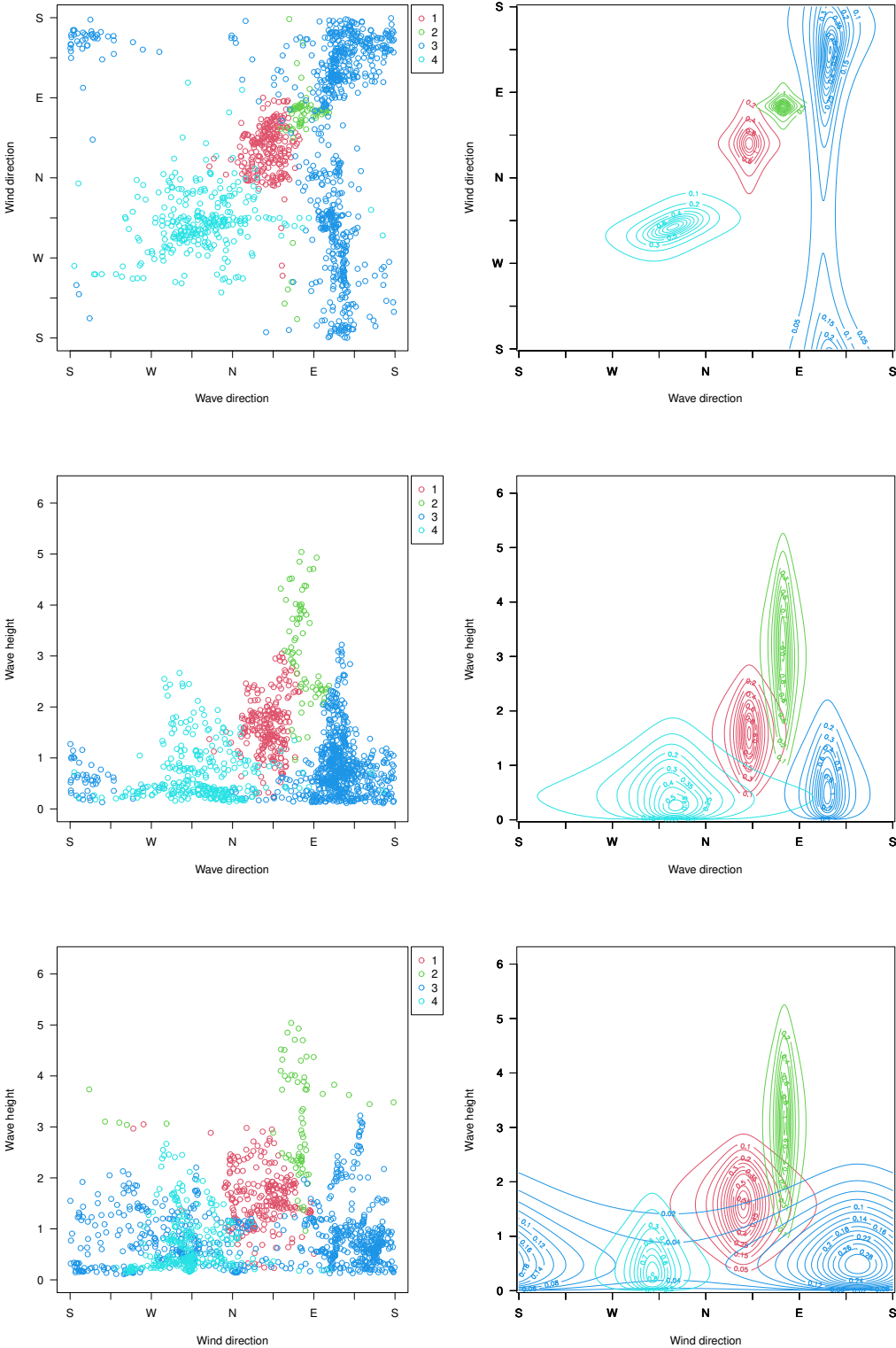
Figure 5: Contour plots for the climate data of the bivariate marginal distributions of our extended TWCC for the four different clusters as detected by our variant of the EM algorithm. Each cluster is presented in a different colour and N, E, S, W represent north, east, south and west, respectively.

The trivariate wrapped Cauchy copula can be extended in various directions, of which we shall briefly outline four.

- First, we might wish to introduce asymmetry into our copula TWCC(ρ). Skewness can be handled at the level of the marginals via suitably choosing skew marginal distributions, but this does not allow altering the symmetry of the dependence structure, hence the copula itself. For example, this can be done by adopting the approach of [2] which consists in multiplying (5) with the skewing function $(1 + \lambda_1 \sin(u_1) + \lambda_2 \sin(u_2) + \lambda_3 \sin(u_3))$ for $\lambda_1, \lambda_2, \lambda_3 \in (-1, 1)$ satisfying $|\lambda_1 + \lambda_2 + \lambda_3| < 1$. When all three skewness parameters are 0, we retrieve the original copula, and as soon as one parameter deviates from zero, we obtain a skew version of our TWCC(ρ) given by (5). As future work, it will be interesting to see in how far asymmetry in the copula can add flexibility on top of asymmetry in the marginals, and how both can be ideally combined.

- Second, in a similar manner as in [60], the extended model (28) can be used to construct an AR(2) process on the circle. Let $\Theta_0, \Theta_1, \ldots, \Theta_t$ be $[0, 2\pi)$-valued random variables on the circle such that

$$p(\theta_0, \theta_1) = f(\theta_0, \theta_1),$$

$$p(\theta_t|\theta_{t-1}, \ldots, \theta_0) = p(\theta_t|\theta_{t-1}, \theta_{t-2}) = \frac{|1 - \delta_t^2|}{1 + \delta_t^2 - 2\delta_t \cos(2\pi F(\theta_t) - \eta_t)} f(\theta_t), \tag{34}$$

where $p(\theta_0, \theta_1)$ is the initial distribution and $p(\theta_t|\theta_{t-1}, \theta_{t-2})$ is the transition density. Here $f(\theta_t)$ is a density on the circle $[0, 2\pi)$, $F(\theta_t) = \int_c^{\theta_t} f(x) dx$ for some arbitrary origin c on the circle, and $f(\theta_0, \theta_1)$ is a density on the torus $[0, 2\pi)^2$ with a common univariate marginal density f. Also, the parameters are assumed to satisfy $\eta_t = \arg(\phi_t)$, $\delta_t = |\phi_t|$, $\phi_t = -\rho_{t-1,t-2}\{\rho_{t,t-1}^{-1} e^{2\pi i F(\theta_{t-1})} + \rho_{t,t-2}^{-1} e^{2\pi i F(\theta_{t-2})}$, $\rho_{t,t-1}, \rho_{t,t-2}, \rho_{t-1,t-2} \in \mathbb{R}$, $\rho_{t,t-1} \cdot \rho_{t,t-2} \cdot \rho_{t-1,t-2} > 0$, and $|\rho_{jk}| < |\rho_{ij}\rho_{ik}|/(|\rho_{ij}| + |\rho_{ik}|)$ for (i, j, k) a permutation of $(t, t-1, t-2)$. The transition density (34) is derived by substituting $(\theta_t, \theta_{t-1}, \theta_{t-2})$ into $(\theta_1, \theta_2, \theta_3)$ in (28) with the common marginal density f and calculating its univariate conditional density similarly to Theorem 3(iii). Hence it is clear that this circular AR(2) process is stationary. If f is the wrapped Cauchy density (29), then the transition density (34) can also be expressed in closed form without integrals. The tractability of our model would make the circular AR(2) process very appealing and important for time-dependent directional data.

- Third, our model TWCC(ρ) needs a constraint on the ρ's, entailing that all the three parameters cannot be interpreted simultaneously. This limitation can be overcome if we consider a general constant c_1. We refer the reader to Section F in the Appendix for details of such a model. It will allow us to have the three ρ's without constraints but there will be loss in terms of several of the nice properties of the model discussed in this paper.

- Fourth and finally, it is natural albeit highly challenging to extend the model presented here to any d-dimensional torus. A potential model could be of the form

$$t(\boldsymbol{u}; \boldsymbol{\rho}) \propto \left\{ c_4 + 2 \sum_{1 \le i < j \le d} \rho_{ij} \cos(u_i - u_j) \right\}^{-1} \tag{35}$$

where $\boldsymbol{u} = (u_1, \ldots, u_d)'$, $\boldsymbol{\rho} \in \mathbb{R}^{d(d-1)/2}$ contains the parameters $\rho_{ij} \in \mathbb{R}$, which need to satisfy certain conditions and c_4 depends on them. To make this a valid density, c_4 has at least to be equal to $2 \sum_{1 \le i < j \le d} |\rho_{ij}|$, and we need to find the normalizing constant. Note that the general form of (35) has been proposed in [47] Equation (106); no properties were investigated. One of the key properties of the copula (35) is given in the following theorem.

Theorem 9. *Let a $[0, 2\pi)^d$-valued random vector $(U_1, \ldots, U_d)'$ have the probability density function $t_d(\boldsymbol{u})$ for $\boldsymbol{u} = (u_1, \ldots, u_d)'$. Suppose that t_d is a function of $\{u_i - u_j ; 1 \le i < j \le d\}$, namely,*

$$t_d(\boldsymbol{u}) = h(u_1 - u_2, u_1 - u_3, \ldots, u_{d-1} - u_d), \quad 0 \le u_1, \ldots, u_d < 2\pi. \tag{36}$$

Then the following hold for $(U_1, \ldots, U_d)'$.

(i) The marginal distribution of U_i $(1 \le i \le d)$ has the uniform distribution on the circle.

(ii) If $p_1 + \cdots + p_d \ne 0$, the trigonometric moments of order $(p_1, \ldots, p_d)'$ $(p_1, \ldots, p_d \in \mathbb{Z})$ are $E[e^{i(p_1 U_1 + \cdots + p_d U_d)}] = 0$.

Proof. See Section A.12 in the Appendix. □

Note that Theorem 9(ii) is an extension of Theorem 5(i) which provides the trigonometric moments of the TWCC for $p_1 + p_2 + p_3 \ne 0$. These general results make it appealing to work on the extension of TWCC to (35) in the future.

Acknowledgments

Funding

Appendix

A   Proofs

A.1   Technical lemmas

Lemma 1. *For real-valued variables ϕ_1, ϕ_2, ϕ_3, we have that $|\phi_i| > |\phi_j| + |\phi_k|$ for (i, j, k) a certain permutation of $(1, 2, 3)$ if and only if $\phi_1 z_1 + \phi_2 z_2 + \phi_3 z_3 \neq 0$ for all $(z_1, z_2, z_3)' \in \Omega^3$.*

Proof. Let us start with the necessary condition. Without loss of generality, assume that $|\phi_1| > |\phi_2| + |\phi_3|$. Then the (reverse) triangular inequality combined with straightforward calculations yields

$$
\begin{aligned}
|\phi_1 z_1 + \phi_2 z_2 + \phi_3 z_3| &\geq ||\phi_1 z_1| - |\phi_2 z_2 + \phi_3 z_3|| \\
&= ||\phi_1| - |\phi_2 z_2 + \phi_3 z_3|| \\
&= |\phi_1| - |\phi_2 z_2 + \phi_3 z_3| \\
&\geq |\phi_1| - (|\phi_2| + |\phi_3|) \\
&> 0.
\end{aligned}
$$

The sufficient condition requires some more steps. Without loss of generality assume that $\min\{\phi_1, \phi_2, \phi_3\} = \phi_1$. Then $z_1 \neq -\frac{\phi_2 z_2 + \phi_3 z_3}{\phi_1}$ and $|\phi_i/\phi_1| > 1$ for $i = 2, 3$. From the former condition we can deduce that $\left| -\frac{\phi_2 z_2 + \phi_3 z_3}{\phi_1} \right| < 1$ or $\left| -\frac{\phi_2 z_2 + \phi_3 z_3}{\phi_1} \right| > 1$ for all $(z_2, z_3)' \in \Omega^2$. The special choices $z_2 = \mathrm{sgn}(\phi_2/\phi_1) \in \Omega$ and $z_3 = \mathrm{sgn}(\phi_3/\phi_1) \in \Omega$ lead to

$$
\left| -\frac{\phi_2 z_2 + \phi_3 z_3}{\phi_1} \right| = \left| \frac{\phi_2}{\phi_1} \right| + \left| \frac{\phi_3}{\phi_1} \right| > 1
$$

by our second deduction above. Therefore $\left| -\frac{\phi_2 z_2 + \phi_3 z_3}{\phi_1} \right| > 1$ for all $(z_2, z_3)' \in \Omega^2$. Now choose again $z_2 = \mathrm{sgn}(\phi_2/\phi_1) \in \Omega$ but this time $z_3 = -\mathrm{sgn}(\phi_3/\phi_1) \in \Omega$. From our established inequality we thus know that for these choices of z_2, z_3

$$
\left| -\frac{\phi_2 z_2 + \phi_3 z_3}{\phi_1} \right| > 1
$$
$$
\Leftrightarrow \left| \left| \frac{\phi_2}{\phi_1} \right| - \left| \frac{\phi_3}{\phi_1} \right| \right| > 1,
$$

and consequently either $|\phi_2| > |\phi_1| + |\phi_3|$ or $|\phi_3| > |\phi_1| + |\phi_2|$. $\qquad\square$

A.2   Proof of Theorem 1

Proof. In order to prove the theorem, it suffices to see that the function (5) satisfies: (i) $t(\boldsymbol{u}, \boldsymbol{\rho}) \geq 0$ for any $\boldsymbol{u} = (u_1, u_2, u_3)'$ and (ii) $\int_{[0,2\pi)^3} t(\boldsymbol{u}, \boldsymbol{\rho}) du_1 du_2 du_3 = 1$. Usually, proving non-negativity is straightforward, but in this case it requires calculations because of the form of c_1 which contains the parameters ρ_{12}, ρ_{13} and ρ_{23}.

Proof of (i): Without loss of generality, assume $|\rho_{12}| < |\rho_{13}\rho_{23}|/(|\rho_{13}| + |\rho_{23}|)$. We note that

$$c_1 + 2\left\{\rho_{12}\cos(u_1 - u_2) + \rho_{13}\cos(u_1 - u_3) + \rho_{23}\cos(u_2 - u_3)\right\}$$

$$= \left\|\phi_1\begin{pmatrix}\cos u_1 \\ \sin u_1\end{pmatrix} + \phi_2\begin{pmatrix}\cos u_2 \\ \sin u_2\end{pmatrix} + \phi_3\begin{pmatrix}\cos u_3 \\ \sin u_3\end{pmatrix}\right\|^2,$$

where $\phi_i = \text{sgn}(\rho_{jk})(\rho_{ij}\rho_{ik}/\rho_{jk})^{1/2}$, $1 \le i, j, k \le 3$, $j, k \ne i, j < k$. Then

$$\left\|\phi_1\begin{pmatrix}\cos u_1 \\ \sin u_1\end{pmatrix} + \phi_2\begin{pmatrix}\cos u_2 \\ \sin u_2\end{pmatrix} + \phi_3\begin{pmatrix}\cos u_3 \\ \sin u_3\end{pmatrix}\right\|$$

$$\ge \left\|\phi_3\begin{pmatrix}\cos u_3 \\ \sin u_3\end{pmatrix}\right\| - \left\|\phi_1\begin{pmatrix}\cos u_1 \\ \sin u_1\end{pmatrix} + \phi_2\begin{pmatrix}\cos u_2 \\ \sin u_2\end{pmatrix}\right\|$$

$$\ge \sqrt{\frac{\rho_{13}\rho_{23}}{\rho_{12}}} - \left(\sqrt{\frac{\rho_{12}\rho_{13}}{\rho_{23}}} + \sqrt{\frac{\rho_{12}\rho_{23}}{\rho_{13}}}\right)$$

$$> 0. \tag{37}$$

The last inequality follows by showing

$$\frac{\rho_{13}\rho_{23}}{\rho_{12}} - \left(\sqrt{\frac{\rho_{12}\rho_{13}}{\rho_{23}}} + \sqrt{\frac{\rho_{12}\rho_{23}}{\rho_{13}}}\right)^2$$

$$= \frac{1}{\rho_{12}\rho_{13}\rho_{23}}\left\{\rho_{13}^2\rho_{23}^2 - \rho_{12}^2(|\rho_{13}| + |\rho_{23}|)^2\right\}$$

$$> \frac{1}{\rho_{12}\rho_{13}\rho_{23}}\left\{\rho_{13}^2\rho_{23}^2 - \left(\frac{|\rho_{13}\rho_{23}|}{|\rho_{13}| + |\rho_{23}|}\right)^2(|\rho_{13}| + |\rho_{23}|)^2\right\}$$

$$= 0.$$

Therefore $c_1 + 2\left\{\rho_{12}\cos(u_1 - u_2) + \rho_{13}\cos(u_1 - u_3) + \rho_{23}\cos(u_2 - u_3)\right\} > 0$ for any $(u_1, u_2, u_3)'$.

Next we show that the radicand in c_2 is positive. It is straightforward to see that

$$\rho_{12}^2\rho_{13}^2\rho_{23}^2\left(\left(\frac{\rho_{12}\rho_{13}}{\rho_{23}}\right)^2 + \left(\frac{\rho_{12}\rho_{23}}{\rho_{13}}\right)^2 + \left(\frac{\rho_{13}\rho_{23}}{\rho_{12}}\right)^2 - 2\rho_{12}^2 - 2\rho_{13}^2 - 2\rho_{23}^2\right)$$

$$= (\rho_{12}^2 - \rho_{23}^2)^2\left\{\rho_{13}^2 - \frac{\rho_{12}^2\rho_{23}^2(\rho_{12}^2 + \rho_{23}^2)}{(\rho_{12}^2 - \rho_{23}^2)^2}\right\}^2 - \frac{4\rho_{12}^6\rho_{23}^6}{(\rho_{12}^2 - \rho_{23}^2)^2}. \tag{38}$$

It follows from the assumption $|\rho_{12}| < |\rho_{13}\rho_{23}|/(|\rho_{13}| + |\rho_{23}|)$ that $|\rho_{13}| > |\rho_{12}\rho_{23}|/(|\rho_{23}| - |\rho_{12}|)$. Also

$$\rho_{13}^2 > \left(\frac{|\rho_{12}\rho_{23}|}{|\rho_{23}| - |\rho_{12}|}\right)^2.$$

Then the radicand (38) can be evaluated as

$$(\rho_{12}^2 - \rho_{23}^2)^2\left\{\rho_{13}^2 - \frac{\rho_{12}^2\rho_{23}^2(\rho_{12}^2 + \rho_{23}^2)}{(\rho_{12}^2 - \rho_{23}^2)^2}\right\}^2 - \frac{4\rho_{12}^6\rho_{23}^6}{(\rho_{12}^2 - \rho_{23}^2)^2}$$

$$> (\rho_{12}^2 - \rho_{23}^2)^2\left\{\left(\frac{|\rho_{12}\rho_{23}|}{|\rho_{23}| - |\rho_{12}|}\right)^2 - \frac{\rho_{12}^2\rho_{23}^2(\rho_{12}^2 + \rho_{23}^2)}{(\rho_{12}^2 - \rho_{23}^2)^2}\right\}^2 - \frac{4\rho_{12}^6\rho_{23}^6}{(\rho_{12}^2 - \rho_{23}^2)^2}$$

$$= 0.$$

Hence $c_2 > 0$. Thus the function (5) satisfies the condition (i) for $|\rho_{12}| < |\rho_{13}\rho_{23}|/(|\rho_{13}| + |\rho_{23}|)$. Due to the symmetry of the function (5), it immediately follows that the condition (i) holds for the other two cases $|\rho_{13}| < |\rho_{12}\rho_{23}|/(|\rho_{12}| + |\rho_{23}|)$ and $|\rho_{23}| < |\rho_{12}\rho_{13}|/(|\rho_{12}| + |\rho_{13}|)$.

Proof of (ii): In order to see that the function (5) satisfies (ii), we first note the equation (3.613.2.6) of [17], that is,

$$\int_0^{2\pi} \frac{du}{1 + b\cos u} = \frac{2\pi}{|1 - b^2|^{1/2}}, \quad |b| < 1. \tag{39}$$

Using this result, it follows that

$$\int_0^{2\pi} t(\boldsymbol{u}, \boldsymbol{\rho})du_3$$

$$= \int_0^{2\pi} c_2 \Big[c_1 + 2\left\{\rho_{12}\cos(u_1 - u_2) + \rho_{13}\cos(u_1 - u_3) + \rho_{23}\cos(u_2 - u_3)\right\}\Big]^{-1} du_3$$

$$= \frac{c_2}{c_1 + 2\rho_{12}\cos(u_1 - u_2)} \int_0^{2\pi} \left[1 + \frac{2\{\rho_{13}\cos(u_1 - u_3) + \rho_{23}\cos(u_2 - u_3)\}}{c_1 + 2\rho_{12}\cos(u_1 - u_2)}\right]^{-1} du_3$$

$$= \frac{c_2}{c_1 + 2\rho_{12}\cos(u_1 - u_2)} \int_0^{2\pi} \frac{1}{1 + b'\cos(u_3 - a')} du_3$$

$$= \frac{c_2}{c_1 + 2\rho_{12}\cos(u_1 - u_2)} \cdot \frac{2\pi}{|1 - b'^2|^{1/2}}, \tag{40}$$

where $b' = 2\{\rho_{13}^2 + \rho_{23}^2 + 2\rho_{13}\rho_{23}\cos(u_1 - u_2)\}^{1/2}/\{c_1 + 2\rho_{12}\cos(u_1 - u_2)\}$ and a' satisfies $\tan\alpha' = (\rho_{13}\sin u_1 + \rho_{23}\sin u_2)/(\rho_{13}\cos u_1 + \rho_{23}\cos u_2)$. The third equality follows from the formula $\alpha\cos u_3 + \beta\sin u_3 = \sqrt{\alpha^2 + \beta^2}\cos(u_3 - \gamma)$, where γ satisfies $\tan\gamma = \beta/\alpha$ and the fact that we can write

$$\rho_{13}\cos(u_1 - u_3) + \rho_{23}\cos(u_2 - u_3)$$
$$= \cos(u_3)(\rho_{13}\cos(u_1) + \rho_{23}\cos(u_2)) + \sin(u_3)(\rho_{13}\sin(u_1) + \rho_{23}\sin(u_2)).$$

In order to see $|b'| < 1$ in the last equality, it suffices to see that

$$c_1 + 2\rho_{12}\cos(u_1 - u_2) - 2\{\rho_{13}^2 + \rho_{23}^2 + 2\rho_{13}\rho_{23}\cos(u_1 - u_2)\}^{1/2}$$

$$= \left\|\left\|\phi_1\begin{pmatrix}\cos u_1 \\ \sin u_1\end{pmatrix} + \phi_2\begin{pmatrix}\cos u_2 \\ \sin u_2\end{pmatrix}\right\| - \left\|\phi_3\begin{pmatrix}\cos u_3 \\ \sin u_3\end{pmatrix}\right\|\right\|^2$$

$$> 0,$$

holds for any $u_1, u_2, u_3 \in [0, 2\pi)$. If $|\rho_{12}| < |\rho_{13}\rho_{23}|/(|\rho_{13}| + |\rho_{23}|)$, this inequality is already seen in (37). If $|\rho_{13}| < |\rho_{12}\rho_{23}|/(|\rho_{12}| + |\rho_{23}|)$ or $|\rho_{23}| < |\rho_{12}\rho_{13}|/(|\rho_{12}| + |\rho_{13}|)$, we have

$$\left\|\phi_1\begin{pmatrix}\cos u_1 \\ \sin u_1\end{pmatrix} + \phi_2\begin{pmatrix}\cos u_2 \\ \sin u_2\end{pmatrix}\right\| - \left\|\phi_3\begin{pmatrix}\cos u_3 \\ \sin u_3\end{pmatrix}\right\| \geq \left|\sqrt{\frac{\rho_{12}\rho_{13}}{\rho_{23}}} - \sqrt{\frac{\rho_{12}\rho_{23}}{\rho_{13}}}\right| - \sqrt{\frac{\rho_{13}\rho_{23}}{\rho_{12}}} > 0.$$

The last inequality follows from

$$\left|\sqrt{\frac{\rho_{12}\rho_{13}}{\rho_{23}}} - \sqrt{\frac{\rho_{12}\rho_{23}}{\rho_{13}}}\right|^2 - \frac{\rho_{13}\rho_{23}}{\rho_{12}}$$

$$= \frac{1}{\rho_{12}\rho_{13}\rho_{23}}\left[\rho_{12}^2\{\rho_{13} - \rho_{23}\}^2 - \rho_{13}^2\rho_{23}^2\right]$$

$$\geq \frac{1}{\rho_{12}\rho_{13}\rho_{23}}\left\{\rho_{12}^2(|\rho_{13}| - |\rho_{23}|)^2 - \rho_{13}^2\rho_{23}^2\right\}$$

$$> \frac{1}{\rho_{12}\rho_{13}\rho_{23}}\left\{\left(\frac{\rho_{13}\rho_{23}}{|\rho_{13}| - |\rho_{23}|}\right)^2(|\rho_{13}| - |\rho_{23}|)^2 - \rho_{13}^2\rho_{23}^2\right\}$$

$$= 0.$$

Thus we have $c_1 + 2\rho_{12}\cos(u_1 - u_2) - 2\{\rho_{13}^2 + \rho_{23}^2 + 2\rho_{13}\rho_{23}\cos(u_1 - u_2)\}^{1/2} > 0$, which implies $|b'| < 1$.

(40) can be simplified as

$$\int_0^{2\pi} t(\boldsymbol{u}, \boldsymbol{\rho})du_3 = \frac{2\pi \cdot c_2}{|\rho_{12}\rho_{23}/\rho_{13} + \rho_{12}\rho_{13}/\rho_{23} - \rho_{13}\rho_{23}/\rho_{12} + 2\rho_{12}\cos(u_1 - u_2)|} \tag{41}$$
$$\equiv t_2(u_1, u_2; \phi_{12}),$$

where ϕ_{12} is defined in (11). Here we show that the denominator of (41) is positive for any $(u_1, u_2)'$. For convenience, write $c_3 = \rho_{12}\rho_{23}/\rho_{13} + \rho_{12}\rho_{13}/\rho_{23} - \rho_{13}\rho_{23}/\rho_{12}$. Let $\rho_{12} > 0$, and we have the following:

(a) If $|\rho_{12}| < |\rho_{13}\rho_{23}|/(|\rho_{13}| + |\rho_{23}|)$, then

$$c_3 + 2\rho_{12}\cos(u_1 - u_2) \le c_3 + 2\rho_{12} = \frac{\rho_{12}^2(\rho_{13} + \rho_{23})^2 - \rho_{13}^2\rho_{23}^2}{\rho_{12}\rho_{13}\rho_{23}}$$

$$< \frac{1}{\rho_{12}\rho_{13}\rho_{23}}\left[\left(\frac{|\rho_{13}||\rho_{23}|}{|\rho_{13}| + |\rho_{23}|}\right)^2(\rho_{13} + \rho_{23})^2 - \rho_{13}^2\rho_{23}^2\right]$$

$$= \frac{\rho_{13}^2\rho_{23}^2}{\rho_{12}\rho_{13}\rho_{23}}\left[\left(\frac{\rho_{13} + \rho_{23}}{|\rho_{13}| + |\rho_{23}|}\right)^2 - 1\right]$$

$$\le 0.$$

(b) If $|\rho_{13}| < |\rho_{12}\rho_{23}|/(|\rho_{12}| + |\rho_{23}|)$ or $|\rho_{23}| < |\rho_{12}\rho_{13}|/(|\rho_{12}| + |\rho_{13}|)$, we have

$$c_3 + 2\rho_{12}\cos(u_1 - u_2) \ge c_3 - 2\rho_{12} = \frac{\rho_{12}^2(\rho_{23} - \rho_{13})^2 - \rho_{13}^2\rho_{23}^2}{\rho_{12}\rho_{13}\rho_{23}}$$

$$> \frac{1}{\rho_{12}\rho_{13}\rho_{23}}\left[\left(\frac{|\rho_{13}||\rho_{23}|}{|\rho_{23}| - |\rho_{13}|}\right)^2(\rho_{23} - \rho_{13})^2 - \rho_{13}^2\rho_{23}^2\right]$$

$$= \frac{\rho_{13}^2\rho_{23}^2}{\rho_{12}\rho_{13}\rho_{23}}\left[\left(\frac{\rho_{23} - \rho_{13}}{|\rho_{23}| - |\rho_{13}|}\right)^2 - 1\right]$$

$$\ge 0.$$

Next, consider $\rho_{12} < 0$. In this case, if $|\rho_{12}| < |\rho_{13}\rho_{23}|/(|\rho_{13}| + |\rho_{23}|)$, it is straightforward to show $c_3 + 2\rho_{12}\cos(u_1 - u_2) < 0$ in a similar manner as in the case (A.2) except using $|\rho_{13}| + |\rho_{23}| = |\rho_{13} - \rho_{23}|$, which holds as $\rho_{12} < 0$ means that $\rho_{13}\rho_{23} < 0$. If $|\rho_{13}| < |\rho_{12}\rho_{23}|/(|\rho_{12}| + |\rho_{23}|)$ or $|\rho_{23}| < |\rho_{12}\rho_{13}|/(|\rho_{12}| + |\rho_{13}|)$, then we can see that $c_3 + 2\rho_{12}\cos(u_1 - u_2) > 0$ in a similar manner as in the case (A.2) apart from the use of $(\rho_{13} + \rho_{23})^2 = (|\rho_{13}| - |\rho_{23}|)^2$. Thus the denominator of (41) is positive for any $(u_1, u_2)'$.

Note that the discussion above implies $|2\rho_{12}/c_3| < 1$. Then it follows from the equation (3.613.2.6) of [17] that, for the parameters satisfying $c_3 + 2\rho_{12}\cos(u_1 - u_2) > 0$,

$$
\begin{aligned}
\int_0^{2\pi} t_2(u_1, u_2; \phi_{12})du_2 &= \int_0^{2\pi} \frac{2\pi c_2}{c_3 + 2\rho_{12}\cos(u_1 - u_2)}du_2 \\
&= \int_0^{2\pi} \frac{2\pi c_2}{c_3\{1 + 2(\rho_{12}/c_3)\cos(u_1 - u_2)\}}du_2 \\
&= \frac{(2\pi)^2 c_2}{c_3|1 - (2\rho_{12}/c_3)^2|^{1/2}} = \frac{(2\pi)^2 c_2}{|c_3^2 - 4\rho_{12}^2|^{1/2}} \\
&= \frac{1}{2\pi}.
\end{aligned}
\tag{42}
$$

Similarly, we can also show $\int_0^{2\pi} t_2(u_1, u_2; \phi_{12})du_2 = 1/(2\pi)$ for the parameters which satisfy $c_3 + 2\rho_{12}\cos(u_1 - u_2) < 0$. Finally,

$$\int_0^{2\pi} t_1(u_1)du_1 = \int_0^{2\pi} \frac{1}{2\pi}du_1 = 1.$$

Thus the proposed density (5) satisfies the condition (ii) as required.

Since the function (5) satisfies both conditions (i) and (ii), this function is a probability density function on $[0, 2\pi)^3$. $\square$

A.3 Proof of Proposition 1

Proof. Let $\boldsymbol{\rho} = (\rho_{12}, \rho_{13}, \rho_{23})'$ and $\tilde{\boldsymbol{\rho}} = (\tilde{\rho}_{12}, \tilde{\rho}_{13}, \tilde{\rho}_{23})'$ be two different points in the constrained parameter space of the proposed family (5) with $\rho_{12}\rho_{13}\rho_{23} = \tilde{\rho}_{12}\tilde{\rho}_{13}\tilde{\rho}_{23} = \beta$. Assume that $\boldsymbol{\rho}$ and $\tilde{\boldsymbol{\rho}}$ represent the same distribution, namely, $t(\boldsymbol{u}; \boldsymbol{\rho}) = t(\boldsymbol{u}; \tilde{\boldsymbol{\rho}})$ for any $\boldsymbol{u} = (u_1, u_2, u_3)' \in [0, 2\pi)^3$, where c is the density (5). This implies that there exist real-valued constants C and D such that, for any $\boldsymbol{u} \in [0, 2\pi)^3$,

$$
\begin{aligned}
\rho_{12}&\cos(u_1 - u_2) + \rho_{13}\cos(u_1 - u_3) + \rho_{23}\cos(u_2 - u_3) \\
&= D + C\left\{\tilde{\rho}_{12}\cos(u_1 - u_2) + \tilde{\rho}_{13}\cos(u_1 - u_3) + \tilde{\rho}_{23}\cos(u_2 - u_3)\right\}.
\end{aligned}
$$

Choosing $(u_1, u_2, u_3)'$ equal to $(0, \pi/2, \pi/2)'$, $(\pi/2, 0, \pi/2)'$ and $(\pi/2, \pi/2, 0)'$, respectively, yields, $\rho_{ij} = D + C\tilde{\rho}_{ij}$ for each couple $(i, j) \in \{(1, 2), (1, 3), (2, 3)\}$. Moreover, $(u_1, u_2, u_3)' = (0, 0, 0)'$ gives $\rho_{12} + \rho_{13} + \rho_{23} = D + C(\tilde{\rho}_{12} + \tilde{\rho}_{13} + \tilde{\rho}_{23})$. Summing the first two equalities and subtracting the last entails $0 = 2D$ and hence $D = 0$, leading to

$$\rho_{12}\cos(u_1 - u_2) + \rho_{13}\cos(u_1 - u_3) + \rho_{23}\cos(u_2 - u_3)$$
$$= C\left\{\tilde{\rho}_{12}\cos(u_1 - u_2) + \tilde{\rho}_{13}\cos(u_1 - u_3) + \tilde{\rho}_{23}\cos(u_2 - u_3)\right\}.$$

Then it follows that, for any (u_1, u_2, u_3),

$$(\rho_{12} - C\tilde{\rho}_{12})\cos(u_1 - u_2) + (\rho_{13} - C\tilde{\rho}_{13})\cos(u_1 - u_3) + (\rho_{23} - C\tilde{\rho}_{23})\cos(u_2 - u_3) = 0.$$

Thus

$$\rho_{12} = C\tilde{\rho}_{12}, \ \rho_{13} = C\tilde{\rho}_{13}, \ \rho_{23} = C\tilde{\rho}_{23}.$$

Using this equation and the assumption $\rho_{12}\rho_{13}\rho_{23} = \tilde{\rho}_{12}\tilde{\rho}_{13}\tilde{\rho}_{23} = \beta$, we have

$$\beta = \rho_{12}\rho_{13}\rho_{23} = C^3\tilde{\rho}_{12}\tilde{\rho}_{13}\tilde{\rho}_{23} = C^3\beta.$$

Thus we have $C = 1$. This implies $\boldsymbol{\rho} = \tilde{\boldsymbol{\rho}}$, which is contradictory to the assumption $\boldsymbol{\rho}$ and $\tilde{\boldsymbol{\rho}}$ are two different points. $\qquad\square$

A.4   Proof of Theorem 2

Proof. Without loss of generality, we prove the case $(i, j) = (1, 2)$. The other cases can be shown in a similar manner.

1. It follows from the equation (41) in Section A.2 that the marginal density of $(U_1, U_2)'$ can be expressed as

$$t_2(u_1, u_2; \phi_{12}) = \int_0^{2\pi} t(\boldsymbol{u}, \boldsymbol{\rho})du_3$$
$$= \frac{2\pi \cdot c_2}{|\rho_{12}\rho_{23}/\rho_{13} + \rho_{12}\rho_{13}/\rho_{23} - \rho_{13}\rho_{23}/\rho_{12} + 2\rho_{12}\cos(u_1 - u_2)|}.$$

   This marginal density can be rewritten as

$$t_2(u_1, u_2; \phi_{12}) = \frac{1}{(2\pi)^2}\frac{|1 - \phi_{12}^2|}{1 + \phi_{12}^2 - 2\phi_{12}\cos(u_1 - u_2)}.$$

   The value of ϕ_{12} can be obtained as a solution to the equations $1 + \phi_{12}^2 = C \cdot (\rho_{12}\rho_{23}/\rho_{13} + \rho_{12}\rho_{13}/\rho_{23} - \rho_{13}\rho_{23}/\rho_{12})$ and $-2\phi_{12} = 2C\rho_{12}$ for some $C \neq 0$. Specifically, since these equations imply

$$-\frac{1 + \phi_{12}^2}{2\phi_{12}} = \frac{c_3}{2\rho_{12}}, \tag{43}$$

   where $c_3 = \rho_{12}\rho_{23}/\rho_{13} + \rho_{12}\rho_{13}/\rho_{23} - \rho_{13}\rho_{23}/\rho_{12}$, the solutions of this equation, say $\tilde{\phi}_{12}$, are given by

$$\tilde{\phi}_{12} = \frac{-c_3 \pm \{c_3^2 - 4\rho_{12}^2\}^{1/2}}{2\rho_{12}}$$
$$= \frac{\rho_{13}\rho_{23}/\rho_{12} - \rho_{12}\rho_{23}/\rho_{13} - \rho_{12}\rho_{13}/\rho_{23} \pm (2\pi)^3 c_2}{2\rho_{12}}.$$

   Denote these solutions by $\tilde{\phi}_{12}^+ = \{-c_3 + \{c_3^2 - 4\rho_{12}^2\}^{1/2}\}/(2\rho_{12})$ and $\tilde{\phi}_{12}^- = \{-c_3 - \{c_3^2 - 4\rho_{12}^2\}^{1/2}\}/(2\rho_{12})$. Then by definition of ϕ_{12} it is straightforward to see $\tilde{\phi}_{12}^- = \phi_{12}$, $\tilde{\phi}_{12}^+\tilde{\phi}_{12}^- = 1$ and $\tilde{\phi}_{12}^+ = 1/\phi_{12}$. Note that $t_2(u_1, u_2; \phi_{12})$ in equation (10) with the parameter $\phi_{12}(\neq 0)$ satisfies

$$t_2(u_1, u_2; \phi_{12}) = t_2(u_1, u_2; 1/\phi_{12}), \quad 0 \leq u_1, u_2 < 2\pi. \tag{44}$$

   This expression implies that the two solutions of (43), i.e., $\tilde{\phi}_{12}^+$ and $\tilde{\phi}_{12}^-$, correspond to the parameters of the same distribution. Using the parameters derived from the solution $\tilde{\phi}_{12}^-$, we have

$$t_2(u_1, u_2; \phi_{12}) \propto \left\{1 + \phi_{12}^2 - 2\phi_{12}\cos(u_1 - u_2)\right\}^{-1}.$$

   Since the functional form of this marginal density is essentially the same as that of (4), it follows that the marginal density is given by (10) with $(i, j) = (1, 2)$.

2. It immediately follows from equation (42) in Section A.2 that the marginal distribution of U_1 is the uniform distribution on the circle.

$\qquad\square$

A.5   Proof of Theorem 3

Proof. Without loss of generality, we consider the case $(i, j, k) = (1, 2, 3)$.

1. It is straightforward to derive the first expression of the conditional density (15) from the equation $t_{2|1}(u_1, u_2|u_3; \boldsymbol{\rho}) = t(\boldsymbol{u}; \boldsymbol{\rho})/t_1(u_3)$, where $t(\boldsymbol{u}; \boldsymbol{\rho})$ is the trivariate density (5) and $t_1(u_3)$ is the density of U_3, namely, the circular uniform density (see Theorem 2(ii)). The second expression of the conditional density (16) is available by using the equation

$$\cos(u_1 - u_2) = \cos\{u_1 - u_3 - (u_2 - u_3)\}$$
$$= \cos(u_1 - u_3)\cos(u_2 - u_3) + \sin(u_1 - u_3)\sin(u_2 - u_3).$$

   It follows from equation (2) of [31] that the second expression of the conditional density (16) has the same functional form apart from parametrization.

2. Theorem 2 implies that the density of (U_1, U_2) is given by (10) and the density of U_2 is the circular uniform density. Then it follows from the expression $t_{1|1}(u_1|u_2; \phi_{12}) = t_2(u_1, u_2; \phi_{12})/t_1(u_2)$ that the conditional density of U_1 given $U_2 = u_2$ is the wrapped Cauchy density (17).

3. Using the complex expression of the density (13), the conditional density of Z_1 given $(Z_2, Z_3)' = (z_2, z_3)'$ is of the form

$$tc_{1|2}(z_1|z_2, z_3) \propto \left| z_1 + \frac{\phi_2 z_2 + \phi_3 z_3}{\phi_1} \right|^{-2}, \quad z_1 \in \Omega.$$

   Note that the density of the wrapped Cauchy distribution can be expressed as

$$f(z) = \frac{1}{2\pi} \frac{|1 - \delta^2|}{|z - \delta e^{i\eta}|^2}, \quad z \in \Omega,$$

   where $\eta \in \Omega$ is the location parameter and $\delta \geq 0$ is the concentration parameter (see [50]). It follows that the conditional of Z_1 given $(Z_2, Z_3)' = (z_2, z_3)'$ is the wrapped Cauchy distribution with the location parameter $\arg(\phi_{1|23})$ and concentration parameter $|\phi_{1|23}|$, where $\phi_{1|23} = -\phi_1^{-1}(\phi_2 z_2 + \phi_3 z_3) = -\rho_{23}(\rho_{13}^{-1} e^{iu_2} + \rho_{12}^{-1} e^{iu_3})$.

$\square$

A.6   Proof of Theorem 4

Proof. The trivariate density (5) can be decomposed as

$$t(\boldsymbol{u}; \boldsymbol{\rho}) = t_{1|2}(u_3|u_1, u_2; \delta_{3|12})t_{1|1}(u_2|u_1; \phi_{12})t_1(u_1).$$

Theorems 2 and 3 imply that $t_{1|2}(u_3|u_1, u_2; \delta_{3|12})$ is the wrapped Cauchy density (18), $t_{1|1}(u_2|u_1; \phi_{12})$ is also the wrapped Cauchy density (17), and $t_1(u_1)$ is the circular uniform density. This expression implies that the random variate generation from the proposed trivariate distribution (5) is equivalent to that from the circular uniform and wrapped Cauchy distributions.

It is straightforward to see that u_1 computed in Step 2 is a random variate from the circular uniform distribution. In order to generate random variates u_2 and u_3 from the conditional wrapped Cauchy distributions, we apply the following result: if a random variable U follows the circular uniform distribution on $(-\pi, \pi)$, then the random variable defined by

$$\Theta = \eta + 2\arctan\left\{\left(\frac{1 - \delta}{1 + \delta}\right)\tan\left(\frac{U}{2}\right)\right\}$$

has the wrapped Cauchy distribution with location parameter $\eta \in [0, 2\pi)$ and concentration parameter $\delta \in \mathbb{R}^+ \setminus \{1\}$ with density

$$f(\theta) = \frac{1}{2\pi} \frac{|1 - \delta^2|}{1 + \delta^2 - 2\delta\cos(\theta - \eta)}, \quad 0 \leq \theta < 2\pi.$$

See [50] and [31] for details. Using this result, it is straightforward to see that u_2 and u_3 computed in Step 2 are variates from the conditional wrapped Cauchy distributions with location parameters $u_1 + \arg(\phi_{12})$ and $\eta_{3|12}$ and concentration parameters $|\phi_{12}|$ and $\delta_{3|12}$, respectively. $\square$

A.7 Proof of Theorem 5

Proof. Without loss of generality, assume that $(i, j, k) = (1, 2, 3)$, namely, $|\rho_{23}| < |\rho_{12}\rho_{13}|/(|\rho_{12}| + |\rho_{13}|)$.

For convenience, transform the random vector $(U_1, U_2, U_3)'$ into complex form $(Z_1, Z_2, Z_3)' = (e^{iU_1}, e^{iU_2}, e^{iU_3})'$ which has the density (13). It follows from Theorems 2(i) and 3(iii) that the density of $(Z_1, Z_2, Z_3)'$ can be expressed as

$$tc(\boldsymbol{z}, \boldsymbol{\rho}) = tc_2(z_2, z_3; \phi_{23})tc_{1|23}(z_1|z_2, z_3; \delta_{1|23}) = \frac{1}{(2\pi)^3} \frac{|1 - |\phi_{23}|^2|}{|z_2\bar{z}_3 - \phi_{23}|^2} \frac{|1 - |(\phi_2 z_2 + \phi_3 z_3)/\phi_1|^2|}{|z_1 + (\phi_2 z_2 + \phi_3 z_3)/\phi_1|^2}.$$

Then the trigonometric moments can be calculated as

$$
\begin{aligned}
\Phi(p_1, p_2, p_3) &= \int_{\Omega^2} \frac{z_2^{p_2} z_3^{p_3}}{(2\pi)^2} \frac{|1 - |\phi_{23}|^2|}{|z_2\bar{z}_3 - \phi_{23}|^2} \int_{\Omega} z_1^{p_1} \frac{1}{2\pi} \frac{|1 - |(\phi_2 z_2 + \phi_3 z_3)/\phi_1|^2|}{|z_1 + (\phi_2 z_2 + \phi_3 z_3)/\phi_1|^2} dz_1 dz_2 dz_3 \\
&= \int_{\Omega^2} \frac{z_2^{p_2} z_3^{p_3}}{(2\pi)^2} \frac{|1 - |\phi_{23}|^2|}{|z_2\bar{z}_3 - \phi_{23}|^2} \left(-\frac{\phi_2 z_2 + \phi_3 z_3}{\phi_1} \right)^{p_1} dz_2 dz_3 \\
&= \frac{1}{(2\pi)^2} \sum_{n=0}^{p_1} \binom{p_1}{n} \left(-\frac{\phi_2}{\phi_1} \right)^n \left(-\frac{\phi_3}{\phi_1} \right)^{p_1 - n} \\
&\quad \times \int_{\Omega} z_2^{p_2 + n} z_3^{p_3 + p_1 - n} \frac{|1 - |\phi_{23}|^2|}{|z_2\bar{z}_3 - \phi_{23}|^2} dz_2 dz_3.
\end{aligned}
$$

(45)

The second equality follows from Section 1.4 of [50] and

$$\left| \frac{-(\phi_2 z_2 + \phi_3 z_3)}{\phi_1} \right| \leq \frac{|\phi_2| + |\phi_3|}{|\phi_1|} = |\rho_{23}| \frac{|\rho_{12}| + |\rho_{13}|}{|\rho_{12}\rho_{13}|} < 1.$$

The integration in (45) can be calculated using equation (4.3) of [29] and equation (44) of Section A.4 as

$$\frac{1}{(2\pi)^2} \int_{\Omega} z_2^{p_2 + n} z_3^{p_3 + p_1 - n} \frac{|1 - |\phi_{23}|^2|}{|z_2\bar{z}_3 - \phi_{23}|^2} dz_2 dz_3 = \begin{cases} \varphi_{23}^{|p_2 + n|}, & p_1 + p_2 + p_3 = 0, \\ 0, & p_1 + p_2 + p_3 \neq 0, \end{cases}$$

where $\varphi_{23} = \min\{|\phi_{23}|, |\phi_{23}|^{-1}\}\phi_{23}/|\phi_{23}|$. Then it follows that $\Phi(p_1, p_2, p_3) = 0$ if $p_1 + p_2 + p_3 \neq 0$ and therefore (i) is proved. If $p_1 + p_2 + p_3 = 0$, we have

$$
\begin{aligned}
\Phi(p_1, p_2, p_3) &= \sum_{n=0}^{p_1} \binom{p_1}{n} \left(-\frac{\phi_2}{\phi_1} \right)^n \left(-\frac{\phi_3}{\phi_1} \right)^{p_1 - n} \varphi_{23}^{|p_2 + n|} \\
&= (-\rho_{23})^{p_1} \sum_{n=0}^{p_1} \binom{p_1}{n} \rho_{13}^{-n} \rho_{12}^{-p_1 + n} \varphi_{23}^{|p_2 + n|}
\end{aligned}
$$

as required in (ii). The second equality follows from the equation $-\phi_i/\phi_1 = -\text{sgn}(\rho_{1j})|\rho_{23}| / \{\text{sgn}(\rho_{23})|\rho_{1j}|\} = -\rho_{23}/\rho_{1j}$, where $i, j = 2, 3$, $i \neq j$. In particular, if the additional assumption $p_2 \geq 0$ holds, the binomial theorem implies

$$
\begin{aligned}
&\Phi(p_1, p_2, p_3) \\
&= \sum_{n=0}^{p_1} \binom{p_1}{n} \left(-\frac{\phi_2}{\phi_1} \right)^n \left(-\frac{\phi_3}{\phi_1} \right)^{p_1 - n} \varphi_{23}^{p_2 + n} \\
&= \varphi_{23}^{p_2} (-\rho_{23})^{p_1} \sum_{n=0}^{p_1} \binom{p_1}{n} \left(\frac{\varphi_{23}}{\rho_{13}} \right)^n \left(\frac{1}{\rho_{12}} \right)^{p_1 - n} = \varphi_{23}^{p_2} \left\{ -\rho_{23} \left(\frac{\varphi_{23}}{\rho_{13}} + \frac{1}{\rho_{12}} \right) \right\}^{p_1}.
\end{aligned}
$$

Similarly, for $p_2 \leq -p_1$, we have

$$
\begin{aligned}
\Phi(p_1, p_2, p_3) &= \sum_{n=0}^{p_1} \binom{p_1}{n} \left(-\frac{\phi_2}{\phi_1} \right)^n \left(-\frac{\phi_3}{\phi_1} \right)^{p_1 - n} \varphi_{23}^{-(p_2 + n)} \\
&= \varphi_{23}^{-p_2} \left\{ -\rho_{23} \left(\frac{1}{\varphi_{23}\rho_{13}} + \frac{1}{\rho_{12}} \right) \right\}^{p_1},
\end{aligned}
$$

which gives (iii). Item (iv) of the theorem holds because

$$
\begin{aligned}
\Phi(-p_1, -p_2, -p_3) &= E[e^{-i(p_1 U_1 + p_2 U_2 + p_3 U_3)}] = \overline{E[e^{i(p_1 U_1 + p_2 U_2 + p_3 U_3)}]} \\
&= E[e^{i(p_1 U_1 + p_2 U_2 + p_3 U_3)}] = \Phi(p_1, p_2, p_3).
\end{aligned}
$$

Finally, it is straightforward to show (v) by substituting $p_1 = 0$ in (ii). $\qquad\square$

[31] obtained the expression for the trigonometric moments of the bivariate wrapped Cauchy distribution using the residue theorem. Following the approach given in the proof of Theorem 2 of their paper, it is also possible to express the trigonometric moments in the setting (ii) using the residues. However, for our model, the expression (20) seems more practical because this expression does not involve the calculation of derivatives which appear in the residues.

A.8 Proof of Theorem 6

Proof. If follows from Theorem 2(i) that $(U_i, U_j)'$ has the density (10). This density is equivalent to a special case of the distribution of [31] with circular uniform marginals. Then the three correlation coefficients ρ_{JW}, ρ_{JM} and ρ_{FL} of our model can be immediately calculated from those of the distribution of [31] given in Section 2.6 of their paper. $\square$

A.9 Proof of Theorem 7

Proof. First we consider the case $\rho_{ij}, \rho_{ik}, \rho_{jk} > 0$. Without loss of generality, assume $(i, j, k) = (1, 2, 3)$. It is clear that the antimodes of the density (5) are $u_1 = u_2 = u_3$ because $\cos(u_i - u_j)$ $(1 \leq i < j \leq 3)$ is maximized at $u_i = u_j$. In order to derive the modes of the density (5), we first note that the density (5) can be expressed as

$$t(\boldsymbol{u}, \boldsymbol{\rho}) \propto \left[c_1 + 2\rho_{12}\cos(u_1 - u_2) + 2\{\rho_{13}^2 + \rho_{23}^2 + 2\rho_{13}\rho_{23}\cos(u_1 - u_2)\}^{1/2}\cos(u_3 - \tilde{\eta}_{3|12}) \right]^{-1},$$

where $\tilde{\eta}_{3|12} = \arg\{\rho_{13}\cos u_1 + \rho_{23}\cos u_2 + \mathrm{i}(\rho_{13}\sin u_1 + \rho_{23}\sin u_2)\}$. It immediately follows from this expression that the density (5) is maximized at $u_3 = \tilde{\eta}_{3|12} + \pi$. Then the maximization of the density (5) reduces to the minimization of its functional part

$$B(x) = \rho_{12}x - \{\rho_{13}^2 + \rho_{23}^2 + 2\rho_{13}\rho_{23}x\}^{1/2},$$

where $x = \cos(u_1 - u_2) \in [-1, 1]$. The first derivative of this function is

$$\frac{d}{dx}B(x) = \rho_{12} - \rho_{13}\rho_{23}(\rho_{13}^2 + \rho_{23}^2 + 2\rho_{13}\rho_{23}x)^{-1/2}. \tag{46}$$

Now it is straightforward to see that this derivative can be upper bounded by $\rho_{12} - \rho_{13}\rho_{23}/(\rho_{13} + \rho_{23})$ (by replacing x with 1 in (46)), and that the derivative is thus negative if $\rho_{12} < \rho_{13}\rho_{23}/(\rho_{13} + \rho_{23})$, leading to a minimization of $B(x)$ at $x = 1$ if $\rho_{12} < \rho_{13}\rho_{23}/(\rho_{13} + \rho_{23})$. By using similar arguments, one can show that $B(x)$ is minimized at $x = -1$ if $\rho_{12} > \rho_{13}\rho_{23}/|\rho_{13} - \rho_{23}|$. It then follows that the modes of the density (5) are given at $u_1 = u_2$ for $\rho_{12} < \rho_{13}\rho_{23}/(\rho_{13} + \rho_{23})$ and at $u_1 = u_2 + \pi$ for $\rho_{12} > \rho_{13}\rho_{23}/|\rho_{13} - \rho_{23}|$. Finally, $u_3 = \tilde{\eta}_{3|12} + \pi$ implies that $u_3 = u_1 + \pi$ if $\rho_{12} < \rho_{13}\rho_{23}/(\rho_{13} + \rho_{23})$. If $\rho_{12} > \rho_{13}\rho_{23}/|\rho_{13} - \rho_{23}|$, then we have $u_3 = u_1$ for $\rho_{13} - \rho_{23} < 0$. Noticing that $\rho_{12} > \rho_{13}\rho_{23}/|\rho_{13} - \rho_{23}|$ and $\rho_{13} - \rho_{23} < 0$ imply $\rho_{13} < \rho_{12}\rho_{23}/(\rho_{12} + \rho_{23})$, we obtain the modes of the density (5) for the case $(i, j, k) = (1, 2, 3)$. If $\rho_{12} > \rho_{13}\rho_{23}/|\rho_{13} - \rho_{23}|$ and $\rho_{13} - \rho_{23} > 0$, the modes of the density (5) can be obtained by setting $(i, j, k) = (2, 1, 3)$ rather than $(i, j, k) = (1, 2, 3)$ due to the symmetry of the density (5) with respect to the permutation of (ρ_{ik}, ρ_{jk}).

The modes and antimodes of the density (5) for the case $\rho_{ij} > 0$ and $\rho_{ik}, \rho_{jk} < 0$ can be obtained in the same manner by applying Proposition 4(ii).

$\square$

A.10 Proof of Proposition 2

Multiplying $\rho_{23}/(\rho_{12}\rho_{13})$ to both the numerator and denominator of the TWCC density (5), we obtain

$$t(\boldsymbol{u}; \boldsymbol{\rho})$$

$$= \frac{1}{(2\pi)^3} \left[1 + \rho_{23.13}^4 + \left(\frac{\rho_{23}}{\rho_{12}}\right)^4 - 2\rho_{23.13}^2 - 2\left(\frac{\rho_{23}}{\rho_{12}}\right)^2 - 2\left(\rho_{23.13} \cdot \frac{\rho_{23}}{\rho_{12}}\right)^2 \right]^{1/2}$$

$$\bigg/ \left[1 + \rho_{23.13}^2 + \left(\frac{\rho_{23}}{\rho_{12}}\right)^2 + 2\left\{ \rho_{23.13}\cos(u_1 - u_2) + \frac{\rho_{23}}{\rho_{12}}\cos(u_1 - u_3) \right. \right. \tag{47}$$

$$\left. \left. + \rho_{23.13} \cdot \frac{\rho_{23}}{\rho_{12}}\cos(u_2 - u_3) \right\} \right].$$

From this expression, it is straightforward to see that $t(\boldsymbol{u}; \boldsymbol{\rho}) \to 1/(2\pi)^3$ as $\rho_{23} \to 0$, proving (i), and that

$$t(\boldsymbol{u}; \boldsymbol{\rho}) \to \frac{1}{(2\pi)^3}\frac{1 - \rho_{23.13}^2}{1 + \rho_{23.13}^2 + 2\rho_{23.13}\cos(u_1 - u_2)} \quad \text{as} \quad |\rho_{12}| \to \infty,$$

proving (26). Since the parameter constraint (25) implies $|\rho_{23}| < |\rho_{13}|$, we have $|\rho_{23.13}| < 1$. Finally, it follows from the form of the limiting density (26) that U_3 is independent of $(U_1, U_2)'$ and follows the uniform distribution on the circle and that the marginal of $(U_1, U_2)'$ is the bivariate wrapped Cauchy copula BWC$(0, \rho_{23.13})$.

A.11   Proof of Proposition 3

An alternative expression for the density of TWCC$(\boldsymbol{\rho}_n)$ can be obtained by substituting $\boldsymbol{\rho} = \boldsymbol{\rho}_n$ in (47). This expression, along with $\rho_{23,n}/\rho_{13,n} = O(n^{\lambda-\kappa})$ and $\rho_{23,n}/\rho_{12,n} = O(n^{\lambda-\iota})$, implies that, under the assumption in (i), namely, $\kappa > \lambda$, $t(\boldsymbol{u}; \boldsymbol{\rho}) \to 1/(2\pi)^3$ as $n \to \infty$. If the assumptions in (ii) holds, then we have $\rho_{23,n}/\rho_{13,n} = a$ and $\rho_{23,n}/\rho_{12,n} = a^2 n^{-3/2}$, and hence

$$t(\boldsymbol{u}; \boldsymbol{\rho}) \to \frac{1}{(2\pi)^3} \frac{1-a^2}{1+a^2+2a\cos(u_1-u_2)} \quad \text{as} \quad n \to \infty.$$

This limiting distribution is the distribution (26) with $\rho_{23.13} = a$.

Note that for $a > 0$, the constraint $a < (-1+\sqrt{5})/2$ is necessary to ensure the inequality (25) for any n. This can be seen by first noticing that the inequality (25) implies

$$\frac{1}{1+an^{-3/2}} \cdot \frac{1}{a} \geq 1.$$

Since the left-hand side of this inequality is minimized for $n = 1$, it follows that $1/\{(1+a)a\} \geq 1$. Thus we have $a < (-1+\sqrt{5})/2$.

A.12   Proof of Theorem 9

Proof. (i) Without loss of generality, we calculate the marginal distribution of U_d. The marginal density of U_d can be expressed as

$$f_{u_d}(u_d) = \int_{[0,2\pi)^{d-1}} h(u_1-u_2, u_1-u_3, \ldots, u_{d-1}-u_d) du_1 \cdots du_{d-1}. \tag{48}$$

Putting $v_i = u_i - u_d$ ($i = 1, \ldots, d-1$), it follows that $u_i - u_j = v_i - v_j$ for $j = 1, \ldots, d-1$ and therefore $\{u_i - u_j \,;\, 1 \leq i < j \leq d\}$ can be expressed using $d-1$ variables $v_1, \ldots, v_{d-1}$. Thus the marginal density (48) can be expressed as

$$f_{u_d}(u_d) = \int_{[0,2\pi)^{d-1}} h(v_1-v_2, v_1-v_3, \ldots, v_{d-1}) dv_1 \cdots dv_{d-1} = C.$$

Since $f(u_d)$ is a constant which does not depend on u_d, it follows that the marginal distribution of U_d is the uniform distribution on the circle.

(ii) Using $v_1, \ldots, v_{d-1}$ and u_d, the trigonometric moments of order $(p_1, \ldots, p_d)$ can be expressed as

$$
\begin{aligned}
E\left[e^{i(p_1 U_1 + \cdots p_d U_d)}\right] &= \int_{[0,2\pi)^d} e^{i(p_1 u_1 + \cdots + p_d u_d)} h(u_1, \ldots, u_d) du_1 \cdots du_d \\
&= \int_{[0,2\pi)^d} e^{i\{p_1(v_1+u_d)+\cdots+p_{d-1}(v_{d-1}+u_d)+p_d u_d\}} \\
&\quad \times h(v_1-v_2, v_1-v_3, \ldots, v_{d-1}) dv_1 \cdots dv_{d-1} du_d \\
&= \int_{[0,2\pi)^{d-1}} e^{i(p_1 v_1 + \cdots + p_{d-1} v_{d-1})} h(v_1-v_2, v_1-v_3, \ldots, v_{d-1}) dv_1 \cdots dv_{d-1} \\
&\quad \times \int_{[0,2\pi)} e^{i\{(p_1+\cdots+p_d)u_d\}} du_d.
\end{aligned}
$$

Since $p_1 + \cdots + p_d \neq 0$, we have $\int_{[0,2\pi)} e^{i\{(p_1+\cdots+p_d)u_d\}} du_d = 0$. Therefore

$$E\left[e^{i(p_1 U_1 + \cdots p_d U_d)}\right] = 0.$$

<div align="right">□</div>

B   Reparametrization and additional contour plots of the TWCC density

For a better interpretation of the parameters of the TWCC with the constraint $\rho_{12}\rho_{13}\rho_{23} = 1$, it is advantageous to reparametrize the parameters in terms of reparametrized versions of ρ_{12} and $\rho_{23.13}$ given by

$$\rho_{12}^* = \left\{ \frac{1 - |\rho_{23.13}^*|}{|\rho_{23.13}^*|^{1/2}} \right\}^{2/3} \rho_{12}, \quad \rho_{23.13}^* = \frac{\rho_{23}}{|\rho_{13}|}, \tag{49}$$

respectively. The ranges of these reparametrized parameters are $|\rho_{12}^*| > 1$ and $|\rho_{23.13}^*| > 0$.

Here ρ_{12}^* is called the full dependence parameter. Unlike ρ_{12} itself, ρ_{12}^* has a simpler parameter range and can be directly interpreted without considering the value of $\rho_{23.13}$ or $\rho_{23.13}^*$. The parameter ρ_{12}^* can be derived first by noting that $\rho_{23} = \rho_{23.13} \cdot \rho_{13}$ and the positivity constraint (25) implies $|\rho_{13}| < \{(1 - |\rho_{23.13}|)/|\rho_{23.13}|\}|\rho_{12}|$. In addition it follows from $\rho_{12}\rho_{13}\rho_{23} = 1$ that $|\rho_{13}| = 1/(\rho_{12} \cdot \rho_{23.13})^{1/2}$. Summarizing these results, the range of ρ_{12} can be expressed as $|\rho_{12}| > \{|\rho_{23.13}|^{1/2}/(1 - |\rho_{23.13}|)\}^{2/3}$. Then, in order to achieve a simpler parameter range and maintain its original sign, ρ_{12} can be reparameterized as (49).

The parameter $\rho_{23.13}$ is reparametrized as $\rho_{23.13}^*$ because the original signs of ρ_{13} and ρ_{23} are not uniquely determined by the sign of $\rho_{23.13}$ and the other parameter conditions. For example, $\rho_{23.13} > 0$ implies that both $\rho_{13}, \rho_{23} > 0$ and $\rho_{13}, \rho_{23} < 0$ are possible, and the other parameter conditions do not eliminate either of these possibilities. On the other hand, with the reparametrized parameters ρ_{12}^* and $\rho_{23.13}^*$, there is a one-to-one correspondence between the parameter space of $(\rho_{12}, \rho_{13}, \rho_{23})$ and that of $(\rho_{12}^*, \rho_{23.13}^*)$.

Figure 6 plots the contour plots of the density (5) with $u_3 = 0$ for various combinations of $(\rho_{12}^*, \rho_{23.13}^*)$. Note that the values of the parameters $\rho_{12}^* = -5$ and $\rho_{23.13}^* = 0.1$ in one of the contour plots nearly correspond to those in Figure 1(a) of the main article. The strength of dependence between u_1 and u_2 increases with $|\rho_{23.13}^*|$. Also, as $|\rho_{12}^*|$ increases, the shape of the density becomes closer to the limiting density (26) which has linear contours. It appears that the convergence to the limiting density (26) as $|\rho_{12}^*| \to \infty$ is faster for greater values of $|\rho_{23.13}^*|$. If $|\rho_{12}^*|$ is close to 1, then the TWCC density appears to be more concentrated around $u_1 = 0$.

C   Fisher Information

For ease of presentation, denote $c_2 = \frac{1}{(2\pi)^3} c_4^{1/2}$. Then the expected Fisher Information matrix of the density (5) is given by

$$I(\rho_{12}, \rho_{13}, \rho_{23}) = n \begin{pmatrix} I_{\rho_{12}\rho_{12}} & I_{\rho_{12}\rho_{13}} & I_{\rho_{12}\rho_{23}} \\ I_{\rho_{12}\rho_{13}} & I_{\rho_{13}\rho_{13}} & I_{\rho_{13}\rho_{23}} \\ I_{\rho_{12}\rho_{23}} & I_{\rho_{13}\rho_{23}} & I_{\rho_{23}\rho_{23}} \end{pmatrix}$$

where, denoting (i, j, k) a permutation of $(1, 2, 3)$,

$$I_{\rho_{ij}\rho_{ij}} = \int_{[0,2\pi)^3} -\frac{\partial^2 \log(t(\boldsymbol{u}_m; \boldsymbol{\rho}))}{\partial \rho_{ij}^2} t(\boldsymbol{u}_m; \boldsymbol{\rho}) du_1 du_2 du_3,$$

$$I_{\rho_{ij}\rho_{ik}} = \int_{[0,2\pi)^3} -\frac{\partial^2 \log(t(\boldsymbol{u}_m; \boldsymbol{\rho}))}{\partial \rho_{ij} \partial \rho_{ik}} t(\boldsymbol{u}_m; \boldsymbol{\rho}) du_1 du_2 du_3,$$

and

$$\frac{\partial^2 \log(t(\boldsymbol{u}_m; \boldsymbol{\rho}))}{\partial \rho_{ij}^2} = \frac{\frac{\partial^2 c_2}{\partial \rho_{ij}^2} c_2 - \left(\frac{\partial c_2}{\partial \rho_{ij}}\right)^2}{c_2^2} - \frac{\frac{\partial^2 c_1}{\partial \rho_{ij}^2} F - \left(\frac{\partial c_1}{\partial \rho_{ij}} + 2\cos(u_{im} - u_{jm})\right)^2}{F^2},$$

$$\frac{\partial^2 \log(t(\boldsymbol{u}_m; \boldsymbol{\rho}))}{\partial \rho_{ij} \partial \rho_{ik}}$$

$$= \frac{\frac{\partial^2 c_2}{\partial \rho_{ij} \partial \rho_{ik}} c_2 - \frac{\partial c_2}{\partial \rho_{ij}} \frac{\partial c_2}{\partial \rho_{ik}}}{c_2^2} - \frac{\frac{\partial^2 c_1}{\partial \rho_{ij} \partial \rho_{ik}} F - \left(\frac{\partial c_1}{\partial \rho_{ij}} + 2\cos(u_{im} - u_{jm})\right)\left(\frac{\partial c_1}{\partial \rho_{ik}} + 2\cos(u_{im} - u_{km})\right)}{F^2}.$$

Let us now write out these expressions in detail:

$$F = c_1 + 2\{\rho_{12}\cos(u_{1m} - u_{2m}) + \rho_{13}\cos(u_{1m} - u_{3m}) + \rho_{23}\cos(u_{2m} - u_{3m})\}$$

$$\frac{\partial^2 c_1}{\partial \rho_{ij}^2} = 2\frac{\rho_{ik}\rho_{jk}}{\rho_{ij}^3},$$

$$\frac{\partial^2 c_1}{\partial \rho_{ij}\partial \rho_{ik}} = \frac{1}{\rho_{jk}} - \frac{\rho_{jk}}{\rho_{ik}^2} - \frac{\rho_{jk}}{\rho_{ij}^2},$$

$$\frac{\partial^2 c_2}{\partial \rho_{ij}^2} = \frac{1}{2}\frac{1}{(2\pi)^3}\left(\frac{\partial^2 c_4}{\partial \rho_{ij}^2}c_4^{-1/2} - \frac{1}{2}\left(\frac{\partial c_4}{\partial \rho_{ij}}\right)^2 c_4^{-3/2}\right),$$

$$\frac{\partial c_4}{\partial \rho_{ij}} = 2\rho_{ij}\left(\left(\frac{\rho_{ik}}{\rho_{jk}}\right)^2 + \left(\frac{\rho_{jk}}{\rho_{ik}}\right)^2\right) - 2\frac{(\rho_{jk}\rho_{ik})^2}{\rho_{ij}^3} - 4\rho_{ij},$$

$$\frac{\partial^2 c_4}{\partial \rho_{ij}^2} = 2\left(\frac{\rho_{ik}}{\rho_{jk}}\right)^2 + 2\left(\frac{\rho_{jk}}{\rho_{ik}}\right)^2 + 6\frac{(\rho_{jk}\rho_{ik})^2}{\rho_{ij}^4} - 4,$$

$$\frac{\partial^2 c_2}{\partial \rho_{ij}\partial \rho_{ik}} = \frac{1}{2}\frac{1}{(2\pi)^3}\left(\frac{\partial^2 c_4}{\partial \rho_{ij}\partial \rho_{ik}}c_4^{-1/2} - \frac{1}{2}\frac{\partial c_4}{\partial \rho_{ij}}\frac{\partial c_4}{\partial \rho_{ik}}c_4^{-3/2}\right),$$

$$\frac{\partial^2 c_4}{\partial \rho_{ij}\partial \rho_{ik}} = 4\frac{\rho_{ij}\rho_{ik}}{\rho_{jk}^2} - 4\rho_{ij}\frac{\rho_{jk}^2}{\rho_{ik}^3} - 4\rho_{ik}\frac{\rho_{jk}^2}{\rho_{ij}^3}.$$

D   Simulations

In order to confirm that our MLE algorithm for the trivariate wrapped Cauchy copula from Section 4.2 retrieves the true values of the parameters as the sample size increases, we have conducted a Monte Carlo simulation study. To this end, data has been generated from the copula in (5) using the algorithm described in Theorem 4. The sample sizes considered were 50, 100, 150, 200, 250, 300, 350, 500, 750, 1000, 1250, 1500, 1750, 2000, 3000, 4000, 5000 and for each sample size we made 5000 replications. The median of the results for the different lengths is presented in Figure 7. The true values of the parameters of the copula are $\rho_{12} = 1, \rho_{13} = 0.25$ and $\rho_{23} = 4$ and they are each plotted with dotted lines. For each different sample, the MLE algorithm was repeated with 50 different initial values. The two smaller values converge faster to the truth compared to the larger one. However, the median of the values obtained for all three is close to the true value starting from sample size 500.

Confidence intervals (CIs) for the estimates can be obtained by means of bootstrap. Three different simulation studies were performed, with $B = 200$ bootstrap samples being obtained from a sample of size $n = 100, n = 500$ and $n = 1000$, generated by the distribution with density (5), for parameter values $\rho_{12} = 1, \rho_{13} = -4$ and $\rho_{23} = -0.25$. The estimates of the parameters are obtained by repeating the procedure described in Section 4.2 200 times. The median of the values and the 95% CI for the estimated parameter values are shown in Table 3. The true values of the parameter are included in all bootstrap CIs. For all values of the sample size, the true value is included in the bootstrap CI.

Table 3: The true value of the parameters is reported along with the median and 95% bootstrap confidence interval of the ML estimates of the parameters for 200 bootstrap samples and sample size $n = 100, n = 500$ and $n = 1000$.

Parameter	True value	Median (95% bootstrap CI)		
		$n = 100$	$n = 500$	$n = 1000$
ρ_{12}	1	1.83 (-0.27, 3.96)	0.99 (-0.19, 1.32)	1.06 (0.50, 1.31)
ρ_{13}	-4	-1.92 (-5.26, 0.31)	-3.92 (-8.97, 2.71)	-3.74 (-6.26, -2.63)
ρ_{23}	-0.25	-0.24 (-2.36, 2.33)	-0.26 (-1.12, 0.74)	-0.25 (-0.29, -0.18)

E   Further results for the protein dataset of Section 7.1

For the protein dataset, many marginal distributions were tested as shown in Table 1. The contour plots obtained for the different marginals are presented in Figures 8 to 11.
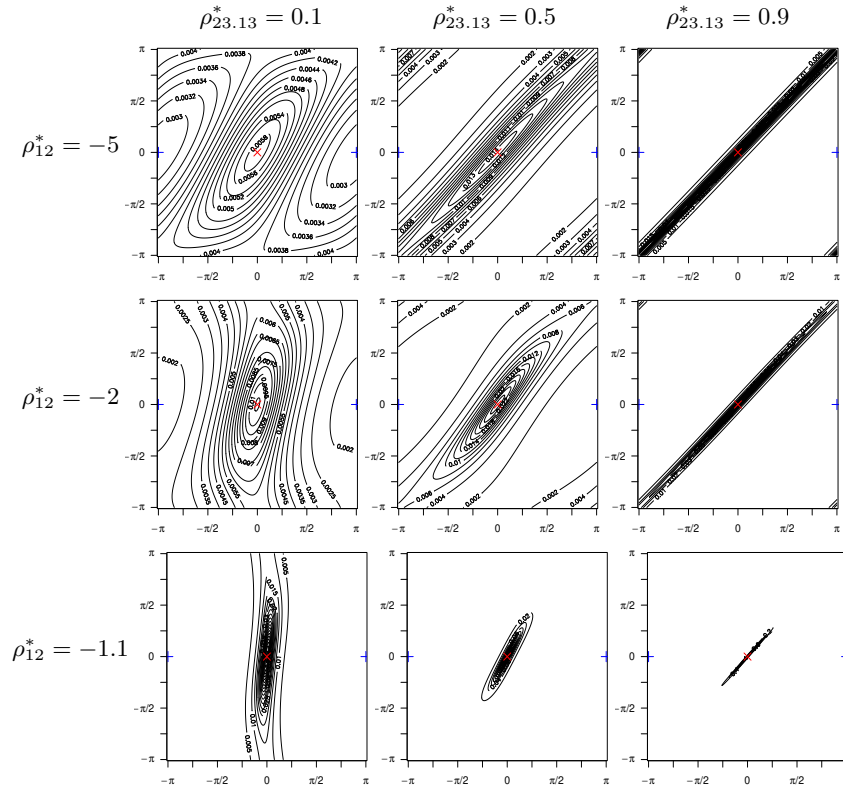
Figure 6: Contour plots of the density of TWCC(ρ) given by (5) with $u_3 = 0$ and $\rho_{12}\rho_{13}\rho_{23} = 1$ for nine combinations of $\left(\rho_{12}^*, \rho_{23.13}^*\right)$, each taking three different values. The horizontal axis represents the value of u_1, while the vertical axis stands for the value of u_2. The symbols '$\times$' (red) and '$+$' (blue) denote the modes and antimodes of density (5), respectively.
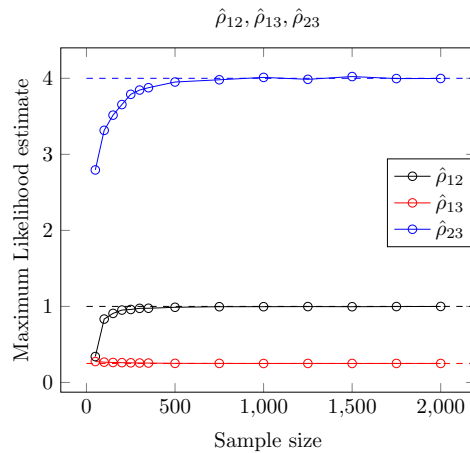

Figure 7: Plots of median values of maximum likelihood estimates for each of the parameters $\rho_{12}, \rho_{13}, \rho_{23}$ from 5000 replications for each sample size. The true parameters, which are plotted with horizontal dotted lines, are $\rho_{12} = 1, \rho_{13} = 0.25$ and $\rho_{23} = 4$.
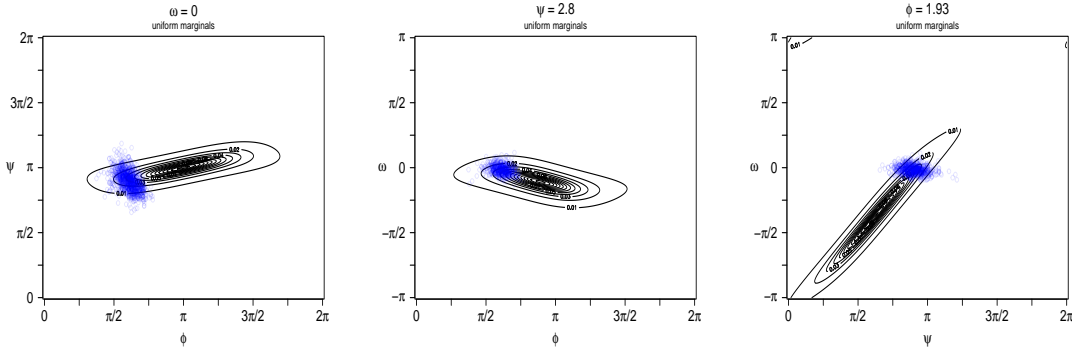
33

Figure 8: Contour plots of density (5) with uniform marginals, with parameter values estimated by maximum likelihood for the protein dataset. The estimates of the copula parameters are $\hat{\rho}_{12} = -0.746, \hat{\rho}_{13} = -0.516, \hat{\rho}_{12} = 2.59$.
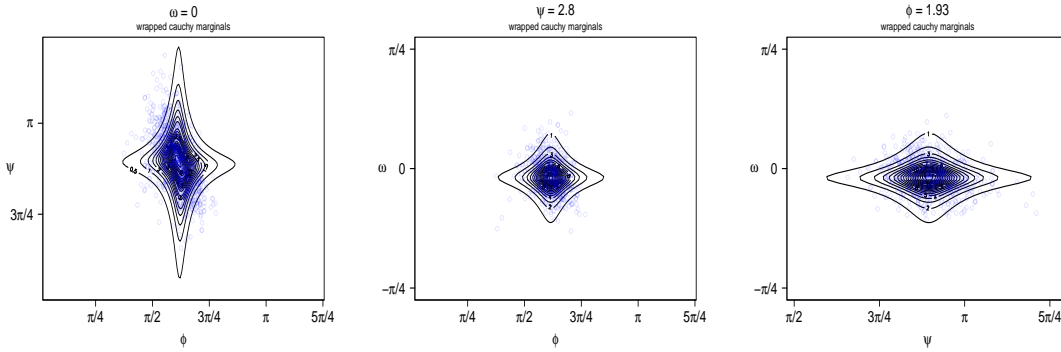

Figure 9: Contour plots of density (5) with wrapped Cauchy marginals, with parameter values estimated by maximum likelihood for the protein dataset. The parameters of the marginals are $\hat{\rho}_1 = 0.89, \hat{\mu}_1 = 1.94, \hat{\rho}_2 = 0.86, \hat{\mu}_2 = 2.80, \hat{\rho}_3 = 0.94, \hat{\mu}_3 = 6.22$, where $\hat{\rho}_i$ and $\hat{\mu}_i$ denote the estimated values for ρ and μ of density (20) corresponding to the density of the marginal distribution of θ_i for $i \in \{1, 2, 3\}$, and the copula parameters are $\hat{\rho}_{12} = 13, \hat{\rho}_{13} = -0.68, \hat{\rho}_{12} = -0.11$.
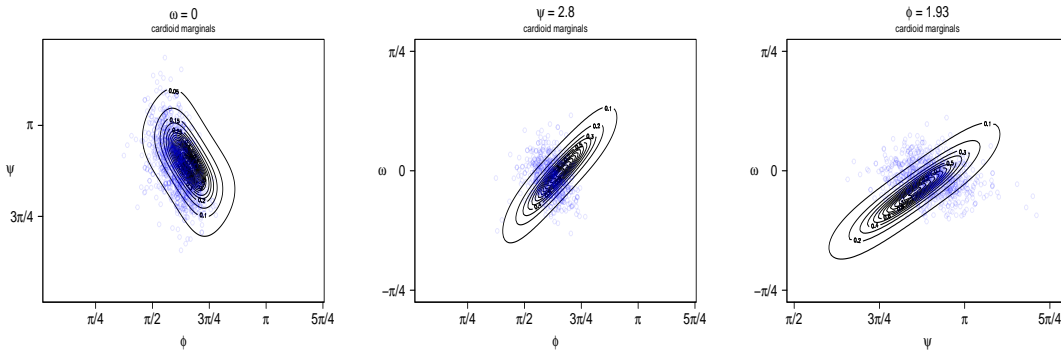

Figure 10: Contour plots of density (5) with cardioid marginals, with parameter values estimated by maximum likelihood for the protein dataset. The parameters of the marginals are $\hat{\rho}_1 = 0.5, \hat{\mu}_1 = 1.93, \hat{\rho}_2 = 0.5, \hat{\mu}_2 = 2.81, \hat{\rho}_3 = 0.5, \hat{\mu}_3 = 0$, where $\hat{\rho}_i$ and $\hat{\mu}_i$ denote the estimated values for ρ and μ of the density $f(\theta; \rho, \mu) = \frac{1}{2\pi}(1 + \rho \cos(\theta - \mu))$ corresponding to the density of the marginal distribution of θ_i for $i \in \{1, 2, 3\}$, and the copula parameters are $\hat{\rho}_{12} = 0.59, \hat{\rho}_{13} = 1.31, \hat{\rho}_{12} = 1.30$.
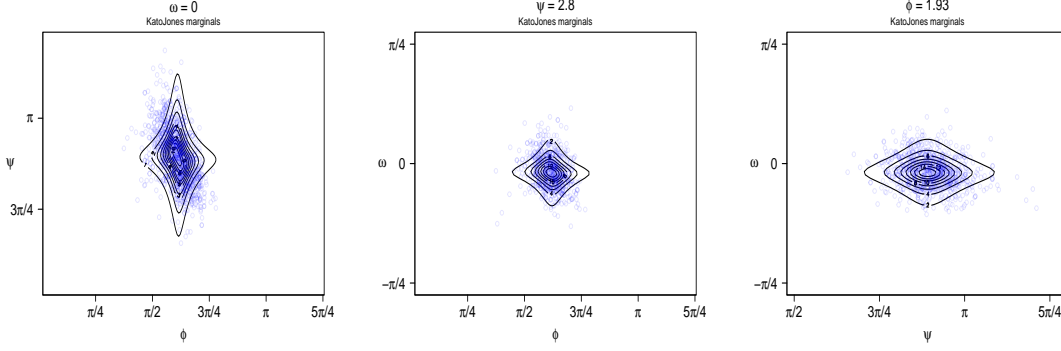
Figure 11: Contour plots of density (5) with Kato–Jones marginals, with parameter values estimated by maximum likelihood for the protein dataset. The parameters of the marginals are $\hat{\mu}_1 = 1.93, \hat{\gamma}_1 = 0.94, \hat{\rho}_1 = 0.88, \hat{\lambda}_1 = 0.004, \hat{\mu}_2 = 2.81, \hat{\gamma}_2 = 0.92, \hat{\rho}_2 = 0.85, \hat{\lambda}_2 = -0.018, \hat{\mu}_3 = 6.23, \hat{\gamma}_3 = 0.97, \hat{\rho}_1 = 0.93, \hat{\lambda}_1 = -0.004$, where $\hat{\rho}_i, \hat{\mu}_i, \hat{\gamma}_i$ and $\hat{\lambda}_i$ denote the estimated values for ρ, μ, γ and λ of the Kato–Jones density as given in [30] corresponding to the density of the marginal distribution of θ_i for $i \in \{1, 2, 3\}$, and the copula parameters are $\hat{\rho}_{12} = 3.24, \hat{\rho}_{13} = 1.49, \hat{\rho}_{12} = 0.21$.

F A generalization of the TWC copula

Here we consider a generalization of the TWC copula (5) to allow for greater flexibility. This generalization can be derived by removing the constraint on c_1 of the density (5) and is given by

$$c(u_1, u_2, u_3) = C_2 \Big[C_1 + 2 \left\{ \rho_{12} \cos(u_1 - u_2) + \rho_{13} \cos(u_1 - u_3) + \rho_{23} \cos(u_2 - u_3) \right\} \Big]^{-1}, \qquad (50)$$

$$0 \le u_1, u_2, u_3 < 2\pi,$$

where $\rho_{12}, \rho_{13}, \rho_{23} \in \mathbb{R}$ satisfy $|\rho_{jk}| < |\rho_{ij}\rho_{ik}|/(|\rho_{ij}| + |\rho_{ik}|)$ for some (i, j, k), that is, a permutation of $(1, 2, 3)$, $C_1 > 2(|\rho_{ij}| + |\rho_{ik}| - |\rho_{jk}|)$, $C_2 = (4\pi)^{-2}\alpha_2[K\{(\alpha_1 + \alpha_2^2/2)^{1/2}/\alpha_2\}]^{-1}$, $\alpha_1 = -C_1^2/2 + 2\rho_{12}^2 + 2\rho_{13}^2 + 2\rho_{23}^2$,

$$\alpha_2 = 2 \left\{ \left(\frac{C_1}{2} + \rho_{12} + \rho_{13} + \rho_{23} \right) \times \prod_{(i,j,k)\in T} \left(\frac{C_1}{2} + \rho_{ij} - \rho_{ik} - \rho_{jk} \right) \right\}^{1/4},$$

$T = \{(1, 2, 3), (1, 3, 2), (2, 3, 1)\}$, and K denotes the complete elliptic integral of the first kind (e.g., [17, equation (8.112.1)]) given by

$$K(\alpha) = \int_0^{\pi/2} \frac{1}{(1 - \alpha^2 \sin^2 t)^{1/2}} dt.$$

If $C_1 = c_1$, then the argument of K in C_2 equals 0 and therefore $C_2 = c_2$. This can be proved as follows. First it can be shown that, with $C_1 = c_1$,

$$\frac{c_1}{2} + \rho_{ij} + q\rho_{ik} + q\rho_{jk} = \frac{(\rho_{ik}\rho_{jk} + q\rho_{ij}\rho_{ik} + q\rho_{ij}\rho_{jk})^2}{2\rho_{12}\rho_{13}\rho_{23}}, \quad q = -1, 1.$$

Hence

$$\alpha_2^2 = 4 \left\{ \left(\frac{c_1}{2} + \rho_{12} + \rho_{13} + \rho_{23} \right) \times \prod_{(i,j,k)\in T} \left(\frac{c_1}{2} + \rho_{ij} - \rho_{ik} - \rho_{jk} \right) \right\}^{1/2}$$

$$= 4 \cdot \frac{1}{4\rho_{12}^2\rho_{13}^2\rho_{23}^2} \left\{ (\rho_{12}\rho_{13} + \rho_{12}\rho_{23} + \rho_{13}\rho_{23}) \times \prod_{(i,j,k)\in T} (\rho_{ik}\rho_{jk} - \rho_{ij}\rho_{ik} - \rho_{ij}\rho_{jk}) \right\},$$

which can be shown to be equal to

$$\alpha_2^2 = c_1^2 - 4\rho_{12}^2 - 4\rho_{13}^2 - 4\rho_{23}^2,$$

so $\alpha_1 + \alpha_2^2/2 = 0$, and the argument of K in C_2 is equal to 0. Hence the normalizing constant reduces to

$$C_2 = \frac{\alpha_2}{(4\pi)^2 K(0)} = \frac{\{c_1^2 - 4\rho_{12}^2 - 4\rho_{13}^2 - 4\rho_{23}^2\}^{1/2}}{(4\pi)^2 \cdot \pi/2} = c_2.$$

It is possible to generalize the model (5) further by lifting the condition on the parameters $|\rho_{jk}| < |\rho_{ij}\rho_{ik}|/(|\rho_{ij}|+|\rho_{ik}|)$. However the domain of C_1 is more involved in that case.

The generalized distribution (50) shares some tractable properties of the distribution (5). For example, the following hold for marginal and conditional distributions of the distribution (50).

Theorem 10. *Let $(U_1, U_2, U_3)'$ follow the distribution (50). Then the following hold for the marginal or conditional distributions of $(U_1, U_2, U_3)'$.*

1. *The marginal distribution of U_i is the uniform distribution on the circle.*

2. *The conditional distribution of $(U_i, U_j)'$ given $U_k = u_k$ is the special case of the distribution of [31] with density (15).*

3. *The conditional distribution of U_i given $(U_j, U_k)' = (u_j, u_k)'$ is the wrapped Cauchy distribution (18).*

Proof. The property (i) is clear from Theorem 9 which will be given in Section A.12. The properties (ii) and (iii) follow immediately from Theorem 3(i) and (iii), respectively, because the generalized density (50) has the same functional form as the density (5). □

It is remarked that differences between the generalized model (50) and the original one (5) are that the marginal distribution of $(U_i, U_j)'$ is not a submodel of [60] and that the conditional distribution of U_i given $U_j = u_j$ is not the wrapped Cauchy in general.

The expressions of modes and antimodes for the generalized density (50) are as simple as those for the original density (5). The proof is straightforward from Theorem (7) and is therefore omitted.

Corollary 1. *The modes and antimodes of the density (50) are the same as those of the density (5) given in Theorem 7.*

Note that this corollary leads to the simplicity of the range of the parameter $C_1 > 2(|\rho_{ij}| + |\rho_{ik}| - |\rho_{jk}|)$.

References

[1] T. Abe and C. Ley. A tractable, parsimonious and flexible model for cylindrical data, with applications. *Econometrics and Statistics*, 4:91–104, 2017.

[2] J. Ameijeiras-Alonso and C. Ley. Sine-skewed toroidal distributions and their application in protein bioinformatics. *Biostatistics*, 23:685–704, 2022.

[3] Y. Baba. Statistics of angular data: wrapped normal distribution model (in japanese). *Proceedings of the Institute of Statistical Mathematics*, 28:41–54, 1981.

[4] D. S. Berkholz, C. M. Driggers, M. V. Shapovalov, R. L. Dunbrack Jr, and P. A. Karplus. Nonplanar peptide bonds in proteins are common and conserved but not biased toward active sites. *Proceedings of the National Academy of Sciences*, 109(2):449–453, 2012.

[5] W. Boomsma, K. V. Mardia, C. C. Taylor, J. Ferkinghoff-Borg, A. Krogh, and T. Hamelryck. A generative, probabilistic model of local protein structure. *Proceedings of the National Academy of Sciences*, 105:8932–8937, 2008.

[6] P. J. A. Cock, T. Antao, J. T. Chang, B. A. Chapman, C. J. Cox, A. Dalke, I. Friedberg, T. Hamelryck, F. Kauff, B. Wilczynski, and M. J. L. de Hoon. Biopython: freely available Python tools for computational molecular biology and bioinformatics. *Bioinformatics (Oxford, England)*, 25(11):1422–1423, 2009.

[7] C. Czado and I. Van Keilegom. Dependent censoring based on parametric copulas. *Biometrika*, 110(3):721–738, 2023.

[8] J. J. Fernández-Durán. Models for circular-linear and circular-circular data constructed from circular distributions based on nonnegative trigonometric sums. *Biometrics*, 63:579–585, 2007.

[9] J. J. Fernández-Durán and M. M. Gregorio-Domínguez. Modeling angles in proteins and circular genomes using multivariate angular distributions based on multiple nonnegative trigonometric sums. *Statistical Applications in Genetics and Molecular Biology*, 13(1):1–18, 2014.

[10] J. J. Fernández-Durán and M. M. Gregorio-Domínguez. CircNNTSR: An R package for the statistical analysis of circular, multivariate circular, and spherical data using nonnegative trigonometric sums. *Journal of Statistical Software*, 70(6):1–19, 2016.

[11] N. I. Fisher and A. J. Lee. A correlation coefficient for circular data. *Biometrika*, 70(2):327–332, 1983.

[12] E. García-Portugués, M. Sörensen, K. V. Mardia, and T. Hamelryck. Langevin diffusions on the torus: estimation and applications. *Statistics and Computing*, 29:1–22, 2019.

[13] C. Genest and A.-C. Favre. Everything you always wanted to know about copula modeling but were afraid to ask. *Journal of Hydrologic Engineering*, 12(4):347–368, 2007.

[14] C. Genest, K. Ghoudi, and L.-P. Rivest. A semiparametric estimation procedure of dependence parameters in multivariate families of distributions. *Biometrika*, 82(3):543–552, 1995.

[15] V. Genna, A. Hospital, and M. Orozco. SARS-CoV-2 Inhibition, Host Selection and Next-Move Prediction Through High-Performance Computing, 2020.

[16] A. Ghalanos and S. Theussl. *Rsolnp: General Non-linear Optimization Using Augmented Lagrange Multiplier Method*, 2015. R package version 1.16.

[17] I. Gradshteyn and I. Ryzhik. *Table of Integrals, Series, and Products, 7th ed.* Academic Press, San Diego, 2007.

[18] T. Hamelryck, K. V. Mardia, and J. Ferkinghoff-Borg, editors. *Bayesian Methods in Structural Bioinformatics*. Springer, Heidelberg, Germany, 2012.

[19] T. Harder, W. Boomsma, M. Paluszewski, J. Frellsen, K. E. Johansson, and T. Hamelryck. Beyond rotamers: a generative, probabilistic model of side chains in proteins. *BMC Bioinformatics*, 11:306, 2010.

[20] A. Jacobsen, E. van Dijk, H. Mouhib, B. Stringer, O. Ivanova, J. Gavaldá-Garciá, L. Hoekstra, K. A. Feenstra, and S. Abeln. Introduction to Protein Structure, 2023.

[21] S. R. Jammalamadaka, A. Sengupta, and A. Sengupta. *Topics in Circular Statistics*. World Scientific, 2001.

[22] H. Joe. *Multivariate Models and Multivariate Dependence Concepts*. Chapman and Hall/CRC, 1997.

[23] H. Joe. *Dependence Modeling with Copulas*. CRC Press, Boca Raton, FL, USA, 2015.

[24] R. A. Johnson and T. E. Wehrly. Measures and models for angular correlation and angular-linear correlation. *Journal of the Royal Statistical Society: Series B (Methodological)*, 39(2):222–229, 1977.

[25] R. A. Johnson and T. E. Wehrly. Some angular-linear distributions and related regression models. *Journal of the American Statistical Association*, 73(363):602–606, 1978.

[26] M. C. Jones, A. Pewsey, and S. Kato. On a class of circulas: copulas for circular distributions. *Annals of the Institute of Statistical Mathematics*, 67:843–862, 2015.

[27] P. E. Jupp and K. V. Mardia. A general correlation coefficient for directional data and related regression problems. *Biometrika*, 67(1):163–173, 1980.

[28] W. Kabsch and C. Sander. Dictionary of protein secondary structure: Pattern recognition of hydrogen-bonded and geometrical features. *Biopolymers*, 22(12):2577–2637, 1983.

[29] S. Kato. A distribution for a pair of unit vectors generated by Brownian motion. *Bernoulli*, 15:898–921, 2009.

[30] S. Kato and M. C. Jones. A tractable and interpretable four-parameter family of unimodal distributions on the circle. *Biometrika*, 102(1):181–190, 2015.

[31] S. Kato and A. Pewsey. A Möbius transformation-induced distribution on the torus. *Biometrika*, 102:359–370, 2015.

[32] S. Kato and K. Shimizu. Dependent models for observations which include angular ones. *Journal of Statistical Planning and Inference*, 138(11):3538–3549, 2008.

[33] S. Kim, A. SenGupta, and B. C. Arnold. A multivariate circular distribution with applications to the protein structure prediction problem. *Journal of Multivariate Analysis*, 143:374–382, 2016.

[34] F. Lagona, M. Picone, and A. Maruotti. A hidden Markov model for the analysis of cylindrical time series. *Environmetrics*, 26(8):534–544, 2015.

[35] T. J. Lane. Protein structure prediction has reached the single-structure frontier. *Nature Methods*, 20(2):170–173, 2023.

[36] C. Ley, S. Babić, and D. Craens. Flexible models for complex data with applications. *Annual Review of Statistics and Its Application*, 8:18.1–18.23, 2021.

[37] C. Ley and T. Verdebout. *Modern Directional Statistics*. Chapman and Hall/CRC Press, Boca Ratón, Florida, 2017.

[38] C. Ley and T. Verdebout, editors. *Applied Directional Statistics: Modern Methods and Case Studies*. Chapman and Hall/CRC Press, Boca Ratón, Florida, 2018.

[39] B. Li and M. G. Genton. Nonparametric identification of copula structures. *Journal of the American Statistical Association*, 108(502):666–675, 2013.

[40] K. Mardia and T. Sutton. A model for cylindrical variables with applications. *Journal of the Royal Statistical Society: Series B (Methodological)*, 40(2):229–233, 1978.

[41] K. V. Mardia. Statistics of directional data. *Journal of the Royal Statistical Society: Series B (Methodological)*, 37:349–371, 1975.

[42] K. V. Mardia. Statistical approaches to three key challenges in protein structural bioinformatics. *Journal of the Royal Statistical Society: Series C (Applied Statistics)*, 62:487–514, 2013.

[43] K. V. Mardia, S. Barber, P. M. Burdett, J. T. Kent, and T. Hamelryck. Mixture Models for Spherical Data with Applications to Protein Bioinformatics. In A. SenGupta and B. C. Arnold, editors, *Directional Statistics for Innovative Applications: A Bicentennial Tribute to Florence Nightingale*, pages 15–32. Springer Nature, Singapore, 2022.

[44] K. V. Mardia, G. Hughes, C. C. Taylor, and H. Singh. A multivariate von Mises distribution with applications to bioinformatics. *Canadian Journal of Statistics*, 36:99–109, 2008.

[45] K. V. Mardia and P. E. Jupp. *Directional Statistics*. John Wiley & Sons, Chichester, United Kingdom, 2000.

[46] K. V. Mardia and C. Ley. Directional distributions. In *Wiley StatsRef: Statistics Reference Online*, pages 1–13. John Wiley & Sons, Ltd, 2018.

[47] K. V. Mardia and K. Sriram. Families of discrete circular distributions with some novel applications. *arXiv*, arXiv:2009.05437, 2020.

[48] K. V. Mardia, C. C. Taylor, and G. K. Subramaniam. Protein bioinformatics and mixtures of bivariate von Mises distributions for angular data. *Biometrics*, 63:505–512, 2007.

[49] G. Mastrantonio. The joint projected normal and skew-normal: A distribution for poly-cylindrical data. *Journal of Multivariate Analysis*, 165:14–26, 2018.

[50] P. McCullagh. Möbius transformation and Cauchy parameter estimation. *The Annals of Statistics*, 24:787–808, 1996.

[51] A. Navarro, J. Frellsen, and R. Turner. The multivariate generalised von Mises distribution: inference and applications. *Proceedings of the Thirty-First AAAI Conference on Artificial Intelligence (AAAI-17)*, pages 2394–2400, 2017.

[52] R. B. Nelsen. *An Introduction to Copulas*. Springer Series in Statistics. Springer, 2nd edition, 2006.

[53] A. Pewsey and E. García-Portugués. Recent advances in directional statistics (with discussion). *TEST*, 30(1):1–58, 2021.

[54] A. Selvitella. On geometric probability distributions on the torus with applications to molecular biology. *Electronic Journal of Statistics*, 13(2):2717 – 2763, 2019.

[55] G. S. Shieh and R. A. Johnson. Inference based on a bivariate distribution with von Mises marginals. *Annals of the Institute of Statistical Mathematics*, 57:789–802, 2005.

[56] G. S. Shieh, S. Zheng, R. A. Johnson, Y. F. Chang, K. Shimizu, C. C. Wang, and S. L. Tang. Modeling and comparing the organization of circular genomes. *Bioinformatics*, 27:912–918, 2011.

[57] H. Singh, V. Hnizdo, and E. Demchuk. Probabilistic model for two dependent circular variables. *Biometrika*, 89:719–723, 2002.

[58] M. Sklar. Fonctions de répartition à n dimensions et leurs marges. *Annales de l'ISUP*, VIII(3):229–231, 1959.

[59] C. B. Thygesen, C. S. Steenmans, A. S. Al-Sibahi, L. S. Moreta, A. B. Sørensen, and T. Hamelryck. Efficient Generative Modelling of Protein Structure Fragments using a Deep Markov Model. In *Proceedings of the 38th International Conference on Machine Learning*, pages 10258–10267. PMLR, 2021.

[60] T. E. Wehrly and R. A. Johnson. Bivariate models for dependence of angular observations and a related Markov process. *Biometrika*, 66:255–256, 1980.